PHYLODYNAMIC QUANTIFICATION OF PATHOGEN TRANSMISSION DYNAMICS

by

Rachel Miller

B.Sc. (Hons), Queen's University, 2017

A THESIS SUBMITTED IN PARTIAL FULFILLMENT OF

THE REQUIREMENTS FOR THE DEGREE OF

MASTER OF SCIENCE

in

THE FACULTY OF GRADUATE AND POSTDOCTORAL STUDIES

(Bioinformatics)

THE UNIVERSITY OF BRITISH COLUMBIA

(Vancouver)

June 2022

The following individuals certify that they have read, and recommend to the Faculty of Graduate and Postdoctoral Studies for acceptance, a thesis entitled:

PHYLODYNAMIC QUANTIFICATION OF PATHOGEN TRANSMISSION DYNAMICS

submitted by Rachel Miller in partial fulfillment of the requirements for

the degree of Master of Science

in Bioinformatics

Examining Committee:

Dr. Jeffrey Joy, Assistant Professor, Department of Medicine, Faculty of Medicine, UBC
Supervisor

Dr. Caroline Colijn, Professor, Department of Mathematics, Faculty of Science, SFU
Supervisory Committee Member

Dr. Matthew Pennell, Associate Professor, Department of Zoology, Faculty of Science, UBC
Supervisory Committee Member

Dr. William Hsiao, Associate Professor, Faculty of Health Sciences, SFU
Additional Examiner

Abstract

As the transmission dynamics of HIV change in response to public health action and other external factors, rapid, scalable and unbiased methods of transmission monitoring become increasingly crucial to gaining and maintaining epidemic control. Analyses of transmission dynamics can direct allocation of public health resources expediently, monitor public health program effectiveness, and identify both existing and developing gaps in prevention. Investigation of lineage-level diversification rate, a phylogenetic approximation of transmission, as a measure for prioritization of transmission clusters for public health intervention was conducted. Both empirical and simulated data were used to compare lineage-level diversification rate-based measures to commonly used non-phylogenetic prioritization measures in ability to statistically separate high and low priority populations, strength of relationship with future growth and number of downstream transmissions produced by prioritized clusters. Further analyses employ phylogenetic methods in the detection of cluster-level transmission changes associated with reductions in access to HIV services related to SARS-CoV-2 restrictions in British Columbia. Cluster growth, branching events and change in lineage-level diversification rates quantify transmission across three sixty-day periods representing “pre-lockdown”, “lockdown” and “post-lockdown”. Results reveal that lineage-level diversification rate-based measures frequently outperform non-phylogenetic measures in prioritizing transmission clusters with the greatest growth potential, while remaining more robust to the effects of missing data. Change in lineage-level diversification rates, in combination with branching events and cluster growth, also indicate increased transmission in clusters associated with people who inject drugs (PWID) relative to clusters associated with men who have sex with men (MSM) during the

period of time following SARS-CoV-2 restriction implementation. Overall, lineage-level diversification rates provide a quantitative and consistent approach to transmission cluster prioritization free of need for external data and aid in the formation of a multi-faceted phylogenetic approach to detecting broader trends in transmission. Phylogenetic methods offer valuable insights crucial to epidemic control in the modern epidemiological landscape of HIV.

Lay Summary

Public health officials faced with more HIV-transmitting groups than can be immediately addressed require an efficient way to identify gaps in prevention and prioritize limited resources in order to maximize their benefit. Existing commonly used methods of transmission monitoring can be hindered by their subjectivity and reliance on historical data, but phylogenetic methods derived purely from viral sequence data can circumvent these faults. Viral sequence data is often collected during routine clinical care and can thus be easily repurposed by phylogenetic methods to approximate transmission magnitude, timing and rate. The work presented in this thesis demonstrates the advantages of employing phylogenetic methods over commonly used non-phylogenetic methods in the prioritization of small groups for public health intervention and reveals the ability of phylogenetic methods that approximate transmission magnitude, timing and rate to detect changes in transmission trends over time.

Preface

Chapters 2 and 3 are based on work conducted by Rachel Miller in the laboratory of Dr. Jeffrey Joy at the British Columbia Centre for Excellence in HIV/AIDS (BC-CfE). Dr. Jeffrey Joy and Rachel Miller are jointly responsible for research project conception and study design. The sequence dataset was collected by the BC-CfE Drug Treatment Program. Transmission cluster inference and calculation of lineage-level diversification rates were conducted using code written by Dr. Jeffrey Joy. Summarization of transmission clusters across bootstrap replicates was conducted using code adapted from a script written by Angela McLaughlin. All other analyses were conducted by Rachel Miller. Work in Chapter 3 was conducted as part of an NSERC CREATE internship hosted virtually by Dr. Tanja Stadler and Dr. Timothy Vaughan. The University of British Columbia – Providence Health Care Research Ethics Board granted ethical approval for the research conducted as part of this thesis (H07- 02559, H17-01812).

Table of Contents

List of Tables

List of Figures

List of Abbreviations

ART: Antiretroviral therapy

BC: British Columbia

BC-CfE: British Columbia Centre for Excellence in HIV/AIDS

DR: Lineage-level diversification rate

FAVITES: Framework for viral transmission and evolution simulation

GTR: Generalized time-reversible

HBV: hepatitis B virus

HCV: hepatitis C virus

HIV: Human immunodeficiency virus

JSD: Jensen-Shannon divergence

LTT: Lineages through time

MSM: Men who have sex with men

OPS: Overdose prevention services

OST: Opioid substitution therapy

PEP: Post-exposure prophylaxis

PrEP: Pre-exposure prophylaxis

PWID: People who inject drugs

SCS: Safe consumption sites

SDRM: Surveillance drug resistance mutation

tMRCA: Time to most recent common ancestor

VL: Viral load

Glossary

Coalescent event: a phylogenetic branching event, where bifurcation from one lineage into two suggests occurrence of a transmission.

Patristic distance: a phylogenetic quantification of the genetic distance between two sequences, calculated as the combined length of the branches separating two tips on a phylogenetic tree.

Phylogeny, phylogenetic tree: A representation of the genetic diversion between sequences, described via the inference of shared common ancestry.

Acknowledgements

First and foremost, I owe huge thanks to my supervisor Dr. Jeffrey Joy, whose expert guidance, ideas and sense of humour have been crucial to the development of my scientific abilities. Further gratitude goes to my supervisory committee, Dr. Caroline Colijn and Dr. Matthew Pennell, for making time to share their valuable insights on my work and for pushing me to think more deeply. I am also grateful to my colleagues Angela McLaughlin, Vince Montoya, Brad Jones and Gideon Mordecai, from whom I have learned very much. Special shoutout to Angela for being my office buddy and mentor. Vince is owed gratitude for his well-timed and much-needed encouragement, as is Dr. Mike Whitlock.

I thank the BC Centre for Excellence in HIV/AIDS, the Canadian Institutes of Health Research, the Natural Science and Engineering Research Council, along with Genome Canada and Genome British Columbia for keeping me funded and financially stable over the course of my degree.

I will always appreciate Dr. Mark Brockman, Dr. Zabrina Brumme and Dr. Gursev Anmole for giving me a chance to start my research career, for teaching me with patience and for continuing to support my journey forward. Lindsay, Mia and Kyle are each deserving of endless gratitude for their friendship, unwavering support and willingness to listen to me complain on a regular basis for the past two and a half years.

Special and enduring thanks go to my parents, brother and grandparents, for their constant support and confidence in me throughout my education. Thank you for making this long and winding path easier to follow. I am lucky to have such positive forces in my life.

Chapter 1: Introduction

1.1 Global challenges in epidemiology and public health

1.1.1 Human-pathogen equilibrium

The evolution of the human population is invariably and intricately linked to the evolution of the pathogens that infect us. Pathogens have always been a threat to human survival and thus a strong selective force, but as modern medicine advances, we become better equipped to dampen the negative effects of pathogen infection. However, as the tools we have to combat infection evolve, concomitantly, we enforce stronger selection on pathogens, forcing them to advance in turn. The evolution of drug resistance illustrates this phenomenon, demonstrating the constant alternation in ability of either modern pharmaceuticals or pathogen mutations to overpower the other[1]. Multiple viral[2,3] and microbial[1] pathogens have developed survival mechanisms in the presence of drugs that could once reliably eliminate them, but the corresponding ability of medical research to develop novel effective drugs perpetuates the cycle. However, as drug-resistance continues to emerge and known mechanisms of treatment not yet blocked by drug-resistance dwindle[1,4,5], infection control measures become the most viable way to actively restrict pathogen spread and its resulting cost to human survival and resources. Thus, methods of monitoring and characterizing the transmission of both existing and emergent pathogens hold significant value, as the insight they provide can allow public health teams to cut transmission chains short before their exponential growth reaches an uncontrollable magnitude.

1.1.2 Modern challenges in pathogen control

As the human population grows and becomes increasingly interconnected, the opportunity for widespread pathogen transmission increases, creating a wider platform for mutation and potential pathogen evolution as traditional infection control methods become progressively more complex and unwieldy. Furthermore, as expansion of the human population drives us to encroach further into previously unoccupied natural ecosystems and stimulate climate change, human-wildlife interactions increase and viral vectors expand their range[6], thus increasing the frequency of opportunity for pathogen mutation[7] and crossover into humans[6,8,9]. Monitoring of pathogen transmission trends already provides a method of focusing limited health resources on populations experiencing elevated transmission, and as the number of pathogens we face increases, such methods will become increasingly critical to the health of human societies.

Additionally, as our control of existing epidemics increases and high-transmission populations shrink, methods of monitoring transmission that enact more fine-grained characterization will be necessary for the advancement of epidemic suppression. Both existing and emergent pathogens pose a threat to the health of human society, and as the modern pathogen landscape develops, methods that allow focused characterization and tracking of pathogen transmission are becoming increasingly valuable.

1.2 The HIV epidemic

1.2.1 The global burden of HIV

Since it's putative crossover into humans in the 1920s[10], HIV has infected an estimated 79.3 million people and been linked to the deaths of 36.3 million, making it a significant global public health challenge[11]. In 2020, the WHO reported that 37.7 million people were living with HIV[11],

although the burden of HIV and level of epidemic control varies markedly between different countries and regions. In regions that facilitate access to antiretroviral therapy (ART), pre-exposure prophylaxis (PrEP), regular HIV diagnostic testing and harm reduction materials such as condoms and safe injection supplies, HIV transmission can be drastically reduced[12]. However, these approaches are not only expensive and difficult to implement quickly, but may also be deprioritized or actively obstructed by policy-makers[13,14]. Even in locations with relatively high levels of epidemic control, such as British Columbia (BC), hundreds of new transmissions are still occurring each year[12], indicating that the methods and allocation of prevention strategies could still be improved.

1.2.2 Methods of HIV treatment and prevention

Well-controlled HIV epidemics are commonly achieved by a comprehensive assortment of treatment and prevention methods[12]. As shown by several studies published in the past decade, individuals who maintain viral suppression via ART have effectively zero risk of transmitting HIV to a sexual partner[15,16], thus making connecting infected individuals with consistent treatment a cornerstone of prevention. The goal of viral suppression also makes regular diagnostic testing critical, as expeditious detection of HIV infection leaves less opportunity for viral replication, therefore shortening the path to suppression. Further elements of prevention include provision of condoms, safe injection supplies, point-of-care testing, PrEP, post-exposure prophylaxis (PEP) and community education. However, providing all of these components is costly and requires time, labour and public health infrastructure to distribute. In order to maximize the benefits of limited resources, many jurisdictions apply prioritization approaches to

the infected and at-risk population in order to focus prevention on groups with the largest potential for downstream negative impact.

1.2.3 The epidemiology of HIV in British Columbia

The HIV epidemic in the province of BC, Canada, is currently relatively well-controlled due to a combination of cohesive public health initiatives. Provision of ART has been consistently increased since 1996[17], with additional efforts to expand ART availability beginning in 2010. Diagnostic testing, viral load testing and drug-resistance testing are part of routine clinical care, as is the provision of harm reduction materials such as condoms and safe infection supplies to at risk individuals. Near real-time phylogenetic monitoring of the local HIV-1 epidemic has been employed since 2013 to detect and prioritize groups with the highest risk of transmission[18]. These focused interventions have allowed public health resources to be allocated with greater efficiency and nearly a decade of using this method to track and respond to the epidemic has contributed to substantial decreases in new HIV diagnoses[12]. Decreasing diagnoses are likely also driven in part by improved access to ART, the expansion of harm reduction strategies[19], and increased uptake of PrEP following the 2018 decision to allow provision to eligible individuals at no cost[20].

1.2.3.1 Data collection by the BC Centre for Excellence in HIV/AIDS

In BC, routine clinical care following every new HIV diagnosis includes drug resistance genotype testing performed by the BC Centre for Excellence in HIV/AIDS (BC-CfE). Viral RNA extracted from patient blood samples is used to amplify and sequence the partial *pol* region of the HIV genome, which is then used to determine which antiretroviral drugs will be most

effective for each individual based on observed viral surveillance drug resistance mutations (SDRMs)[21]. After this information is reported back to the primary care clinicians, the BC-CfE retains both the HIV sequence data and associated metadata. As this process has been part of routine clinical care since 1996, it has led to the creation of a comprehensive dataset representing greater than 75% of the prevalence of HIV in BC[22]. This dataset is extremely valuable because it is repurposed by BC-CfE scientists and local medical health officers to conduct regular molecular monitoring of transmission, thus bypassing what would otherwise be a complex data collection process.

1.3 Molecular epidemiology and HIV

1.3.1 Phylodynamics and viral epidemiology

Viral phylodynamics, the study of the evolutionary forces of selection that influence the structure of viral phylogenies, can provide useful insights highly relevant to public health. Differing population characteristics and trends in transmission will enact differing selection on viral populations, thus creating distinct patterns in the accumulation of genetic variation. Patterns in genetic variation may manifest as differences in phylogenetic branch lengths, clustering or tree balance[23]. Phylodynamic analyses can use such phylogenetic features to make inferences about viral characteristics such as rate of evolution, date of origin or infection, basic reproduction number, geographic spread and strength of selection[23], thus making them an invaluable tool in the epidemiological characterization of many viruses including influenza[24], H1N1[25], hepatitis C virus (HCV)[26], rabies[27], HIV[28] and SARS-CoV-2[29]. Phylodynamics can also be useful in identifying changes in epidemic trends that might signal effectiveness of public health interventions aiming to control viral transmission[23].

1.3.2 Molecular monitoring and transmission cluster inference

Molecular epidemiology, the application of evolutionary patterns derived from population-level pathogen genetic sequence data, provides a route to epidemic monitoring that bypasses several drawbacks of traditional epidemiological methods. Traditional methods that rely on contact tracing, interviews, and assignment of coarse metadata can not only be time consuming, but also prone to error and bias from both the data-collecting and data-providing parties. Pathogen sequence datasets are much less likely to be perturbed by such inaccuracies, and in the case of HIV, often already exist as a byproduct of drug-resistance testing.

Viral pathogen sequence data, in particular HIV sequence data, is amenable to molecular epidemiological methods because viral pathogens constantly accumulate genetic variation. Patterns in genetic variation are heavily influenced by patterns in transmission and selection, and thus the characteristics of a viral epidemic will be reflected in the structure of its' phylogeny. This is particularly true for HIV due to it's rapid rate of evolution, which ensures that viral populations harbored by different individuals rapidly diverge following transmission[30,31].

The level of genetic divergence separating two viral sequences can be phylogenetically quantified via patristic distance, the sum of the lengths of branches linking a pair of tips on a phylogenetic tree. By setting a patristic distance threshold, individuals can be delineated into groups termed "transmission clusters" based on the genetic similarity of the viruses they harbor[32]. The threshold is set such that distances below it are characteristic of distances seen within a single patient and likely indicate relation by recent transmission events if seen between individuals[18]. Importantly, due to the uncertainty introduced by incomplete sampling of the

infected population, phylogenetic methods can never be used to definitively infer transmission directionality between two individuals or cluster members.

Transmission clusters can also be determined non-phylogenetically, by similarly applying a threshold to raw nucleotide distances between pairs of aligned sequences, but this method is hampered by the fact that it doesn't consider the difference between two sequences in the greater evolutionary context of the population of sampled sequences. By ignoring the historic relationships between sequences, non-phylogenetic methods fail to account for differences in evolutionary rate between sites, thus creating opportunity for incorrect assumptions about divergence time[33]. Phylogenetic methods use more of the information available in the alignment by considering how sequences are related by common ancestry[32] and adjusting the distances between them accordingly. Sequence divergence may be better captured by phylogenetic distance matrices, hence giving them an advantage as a starting point for transmission cluster inference. Such advantages have been demonstrated by Balaban *et al*.[34], who showed via simulated data that phylogenetically-defined clusters consistently include individuals with greater transmission potential than clusters defined using genetic distance alone, although the difference is not extreme.

Once a set of transmission clusters has been identified, they provide a mechanism for investigating trends in subsets of the transmitting population that may share non-genetic characteristics. One use of partitioning individuals in this way is that they can be prioritized such that limited public health resources can be allocated most rapidly to clusters with the greatest potential for future growth, in order to quickly quell the greatest number of transmissions before shifting focus to less urgent clusters. Transmission clusters can also be useful on a broader level,

in the investigation of differences in transmission rates between populations characterized by differing attributes of interest such as risk factor, ethnicity, gender or location.

1.3.3 Non-phylogenetic methods of transmission cluster prioritization

Recently, the use of non-phylogenetic measures, either in combination with phylogenetic clustering[18,35], non-phylogenetic clustering[36-38] or without directly considering clustering[39] have been proposed to enhance prioritization processes. The addition of quantitative measures such as cluster size, previous cluster growth, or mean cluster viral load can make the prioritization procedure less subjective. However, there are no established cutoffs defining when such measures reach a level warranting rapid intervention, nor are there established methods for estimating the combined effects of multiple measures. Consequently, cluster prioritization processes remain heavily reliant upon local expertise and subjective interpretation and are thus limited in their ability to be consistent and widely applicable. Furthermore, use of measures such as previous cluster growth or average cluster viral load rely on data collected in previous years or additional linked data, both of which may not always be available. However, phylogenetically derived measures may be able to offer a method of transmission cluster prioritization that circumvents these disadvantages, as they are quantitative and can be calculated consistently from that same dataset used to infer transmission clusters.

1.3.4 Phylogenetic methods of prioritization

The use of phylogenetic methods in prioritization is much less common than the use of non-phylogenetic methods, although recent research[40] provides justification for further development of this field. A method proposed by Moshiri *et al*.[40] that prioritizes individuals based on their

phylogenetic terminal branch lengths was shown to outperform prioritization based on previous transmission cluster growth, demonstrating the potential advantages of using phylogenetic measures in prioritization. However, this method focuses prioritization on individuals rather than transmission clusters, which may be in conflict with ethical considerations and privacy laws in some jurisdictions[41]. Additionally, focusing on individuals rather than groups disregards the context surrounding the individual and may overlook group trends that could inform effective prevention. Furthermore, focusing on terminal branch lengths ignores the historical information contained earlier in the phylogeny and places a coarse threshold on branching that may exclude recent and relevant internal branch lengths. Nevertheless, this method reveals the value of phylogenetic measures of prioritization and validates the exploration of alternative phylogenetic methods that aim to improve upon this starting point.

1.3.5 Lineage-level diversification rate

One possible phylogenetic route to transmission cluster prioritization is through consideration of lineage-level diversification rates. Lineage-level diversification rate is a phylogenetically-derived measure first described by Jetz *et al*.[42] that tracks the historical branching rate of tips in the phylogeny, thus serving as an approximation of transmission rate. Lineage-level diversification rate is the inverse of the equal splits measure, which was initially used to determine genetic distinctness of species in the context of conservation[43].

Lineage-level diversification rate accounts for both the number of branching events and the branch lengths in a phylogenetic tree, and as a tip-weighted measure, it emphasizes recent events. Tips sharing very recent common ancestry with many other lineages will have higher diversification rates, providing evidence for rapid transmission and or increased sampling. The

opposite is true for tips existing in areas of the tree where fewer lineages stem from fewer recent branching events – these tips will have lower diversification rates, suggesting slower transmission rates, or possibly poorer sampling.

Lineage-level diversification rate is advantageous in a prioritization context because it is quantitative, consistent and can be calculated from the sequence data alone, making it a convenient option less likely to be perturbed by human bias. In 2019, McLaughlin *et al*. demonstrated that geographically aggregated lineage-level diversification rates were predictive of new HIV cases[44] and concordant in the identification of clustering risk factors[45], thus making them useful in the detection of populations at high risk for transmission.

1.4 Insight derived from phylogenetic HIV transmission clusters informs public health decisions

1.4.1 Research questions

In this thesis, I investigate the use of phylogenetic methods in the detection of transmission trends relevant to public health decision-making. This work seeks to quantify the strength of the relationship between lineage-level diversification rate and potential future growth of a transmission cluster and identify differences in how well lineage-level diversification rate-based measures and non-phylogenetic measures stratify clusters by future cluster growth potential over time. I also aim to determine differences in how well lineage-level diversification rate-based measures and non-phylogenetic measures stratify clusters by future cluster growth potential at different levels of sampling. The ability of phylogenetic analyses including transmission cluster growth, branching events and lineage-level diversification rate to detect recent changes in cluster transmission associated with changes in epidemiological context is also addressed. Finally, this

work investigates the possibility of differential impacts of SARS-CoV-2 lockdown on transmission in cluster associated with different key population.

1.4.2 Hypotheses

Two main hypotheses motivate the research questions stated above. The first is that HIV transmission cluster prioritization based on phylogenetically derived lineage-level diversification rates will be at least as effective as commonly used non-phylogenetic measures in stratifying clusters by future growth potential, without need for historical data or subjective interpretation. The second hypothesis is that following the initial implementation of SARS-CoV-2 lockdown restrictions and reduced access to HIV management and prevention services in BC, key populations of individuals at risk for HIV will demonstrate differential trends in rates of transmission detectable via phylogenetic analyses that quantitatively approximate transmission preceding, during and following the implementations of restrictions.

Chapter 2: Phylogenetic prioritization of transmission clusters using lineage-level diversification rates

2.1 Introduction

The strategies employed in BC have not only resulted in a more rapid decline in cases relative to other Canadian provinces[46], but have also helped BC make exceptional progress towards the UNAIDS 95-95-95 targets[12,22]. Additionally, phylogenetic monitoring has allowed fine-grained inferences about trends in the BC epidemic, such as the number of new cases joining clusters over time, a metric quantifying local transmission that has consistently declined since 2013 (Figure 2.1C). Although the methods used in BC are highly effective, networks of transmission still exist and more comprehensive characterization and prioritization of transmission groups could improve epidemic control.

Although the addition of quantitative non-phylogenetic measures such as cluster size or previous cluster growth can provide some benefit to prioritization procedures, they can be subjective, inconsistent and reliant on historical data or expert interpretation.

In this chapter, both empirical and simulated data are employed to evaluate the hypothesis that cluster prioritization measures based on phylogenetically-derived lineage-level diversification rates will perform at least equally as well as commonly-used non-phylogenetic prioritization measures in stratifying clusters based on transmission activity, while remaining free of need for additional assumptions, data or historical interpretation. We use BC empirical data to compare phylogenetic diversification rate-based measures to non-phylogenetic measures in their ability to separate clusters labelled by BC public health protocol as “priority” from the

remaining clusters. We further compare prioritization measure performance through a simulation study to reduce the effects of biases that hinder empirical data, such as incomplete sampling and differential cluster intervention. Thus, simulation facilitates direct comparison of the relationship between each prioritization measure and future cluster growth, as well as the direct number of transmissions resulting from prioritized clusters.

2.2 Methods

2.2.1 Empirical data analysis pipeline

The study dataset was restricted to sequence data and linked metadata collected by the BC-CfE between May 1996 and December 2018 inclusive, totaling 35,752 partial *pol* HIV sequences derived from viruses sampled from 9,822 patients. All data were doubly-anonymized prior to analysis. The University of British Columbia – Providence Health Care Research Ethics Board granted ethical approval for this study.

All 35,752 anonymized sequences were aligned with MAFFT v7.310[47]. Known SDRM codons were masked before inference of a phylogenetic tree with 100 bootstraps using FastTree v2.1.10[48]. The full trees were pruned to create 10 subtrees, each containing all sequences collected by the end of each of the 10 years preceding 2019. Each subtree was rooted using the residual-mean-squared function in TempEst v1.5.3[49] and pruned to contain only the earliest sequence available for each individual, leaving 9822 sequences in the largest trees. Transmission clusters were inferred from the full 2018 trees using a patristic distance threshold of 0.02 nucleotide substitutions/site, as described by Poon *et al*.[18], and a 50% bootstrap threshold. The minimum transmission cluster size was set to five individuals to further maintain confidentiality beyond double anonymization of the data. Lineage-level diversification rates were calculated for

all tips in all bootstraps and the median value associated with each tip was kept for use in downstream analyses. In order to quantify the distribution of diversification rates for tips across the 100 bootstraps, the median difference in diversification rate between a tip in a given bootstrap and the same tip in all other bootstraps was calculated. In general, the median difference in diversification rate across bootstraps was very small, although some outlier tips did show greater variation (Figure 2.1).

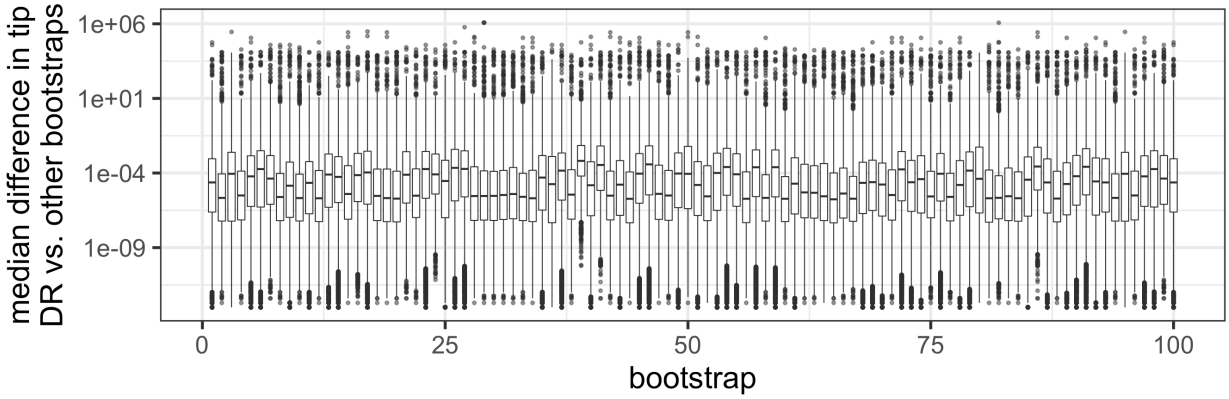

Figure 2.1 Distribution of the median difference diversification rates across bootstraps for each tip. Boxplots represent the median and IQR of the median difference in tip diversification rate in a given bootstrap versus all other bootstraps. In general, the median difference in diversification rate is very small across bootstraps, but some tips show greater variation.

Comparison of cluster median diversification rate to cluster size was also conducted. A positive relationship between median diversification rate across tips in a cluster and cluster size appears to exist at smaller cluster sizes, but weakens as cluster size increases (Figure 2.2), suggesting that elevated diversification rates in larger clusters are not necessarily solely a reflection of increased cluster size.

Figure 2.2 Transmission cluster size versus diversification rate. Each dot represents the median lineage-level diversification rate for a cluster of a particular size. Panel A shows the DR distribution by cluster sizes in the empirical data. Panels B-H show the same, but based on simulated data generated by different parameter sets. Parameter sets include variations from the base set that differ in number of seed individuals, time between infection and the initiation of ART (startART) and the expected degree (Ed) of connectedness within the contact network.

The diversification rate-based measures assessed include cluster mean (MeanDR), median (MedianDR), maximum (MaxDR) and most recent diversification rate (MostRecentDR), as well as the mean of the top three (Top3MeanDR) and top five diversification rates (Top5MeanDR) in a cluster. Non-phylogenetic measures assessed include previous year (PrevYrGrowth), three year (Prev3YrGrowth) and five year growth (PrevYrGrowth), as well as cluster size (ClustSize), previous year cluster growth squared (ClustGrowthSq) and whether or not more than five cases have joined a cluster in the previous year (PrevYr5CasePlus).

The ability of non-phylogenetic measures and diversification rate-based measures to stratify transmission clusters based on transmission activity was evaluated based on the ability of each measure to separate clusters marked as “priority” by the BC public health protocol in a

given year from the remainder. Prioritization decisions made by the BC protocol can be a result of rapid cluster growth, rapid symptom onset seen in one or more cluster members, or combinations of other factors recognized by the public health team as concerning. Successful distinction between these two groups of transmission clusters was assessed using Mann-Whitney U tests.

2.2.2 Epidemic simulation in the FAVITES framework

The need for simulation of the BC epidemic is motivated by two factors. First, intervention decreasing transmission would be expected to reduce lineage-level diversification rate for a transmission cluster, meaning that clusters known to be consistently labelled as priority may display decelerating diversification rates despite having high potential for transmission. Secondly, evaluating novel methods using the set of labels defined by the BC public health protocol as a benchmark assumes that this method accurately captures the true set of clusters with the greatest potential for transmission, which may not necessarily be the case. Simulated epidemics allow evaluation under circumstances where intervention is not applied differentially between clusters and the true clusters with the greatest potential for propagating future transmissions are known.

Simulation was performed using the FAVITES framework[50] to create a contact network, seed infected individuals, generate transmission events and the viral evolution between them, and subsequently sample viral sequences. Simulations were set to run over a 10-year period beginning in 2009, with a base set of parameters adapted from Moshiri *et al.* (2019)[50] and six variations of this set designed to encapsulate a range of reasonable matches to the characteristics of the BC epidemic while still containing enough variation in epidemic parameters to retain

generalizability to epidemics in other locations. Importantly, transmission clusters were not explicitly set or controlled during parameter selection and were instead inferred from the output data following the simulation process. As such, differences occurring in cluster characteristics that drive differences in transmission rate occur as a byproduct of other parameter choices rather than being directly specified and are thus likely to be somewhat inconsistent between replicates. Full description of the parameter selection process can be found in Appendix A.

2.2.3 Simulated data analysis pipeline

For each replicate of each of the seven parameter sets, simulated sequences spanning the full 10-year simulation period were aligned in MAFFT and phylogenies were inferred with FastTree. After rooting on all branches via LSD2[51], each phylogeny was pruned to 10 subtrees, each representing the data collected by the end of a given simulation year. Transmission clusters were inferred for each subtree and lineage-level diversification rates were calculated for all tips. As in the empirical data, a positive relationship between median diversification rate across tips in a cluster and cluster size appears to exist at smaller cluster sizes, but weakens as cluster size increases (Figure 2.2). However, ability to investigate this relationship varies between parameter sets, as parameter configurations vary in the distribution of resulting cluster sizes. Cluster-level prioritization measures were calculated for each subtree such that the Spearman correlation between a prioritization measure in a given year and the amount of cluster growth in a given future year or period of years could be determined and summarized across replicates. Additionally, clusters were ranked by each prioritization measure and individuals from the top clusters (up to inclusion of 100 individuals, or the size of the top cluster, if its size exceeded 100) were used to determine the number of direct resulting transmissions, for comparison to the

number of transmissions produced by a random sample of lower-ranked clusters containing the same number of individuals.

2.3 Results

2.3.1 Empirical data

2.3.1.1 BC HIV Transmission Clusters

The numbers of both clustered and non-clustered cases decreased over time, as did the number of new cases (Figure 2.3C). In more recent years, a larger proportion of the new cases being diagnosed were non-clustered, further suggesting that more sensitive methods will be required to appropriately address all cases going forward. However, clusters capture pockets of closely related transmissions, and as comparison of diversification rates from un-clustered versus clustered tips suggests (Figure 2.4), the potential for rapid transmission is significantly greater within clusters (Mann-Whitney $p < 0.001$), thus rationalizing the focus on these groups as primary public health targets. Even within clusters, hundreds of cases occur each year that could be prevented if the accuracy and resolution of prioritization was increased. The right-tailed log distribution of diversification rates highlights the ability of this measure to allow more focused prioritization, as there are very few diversification rates that are very high relative to the majority of the measurements (Figure 2.3B).

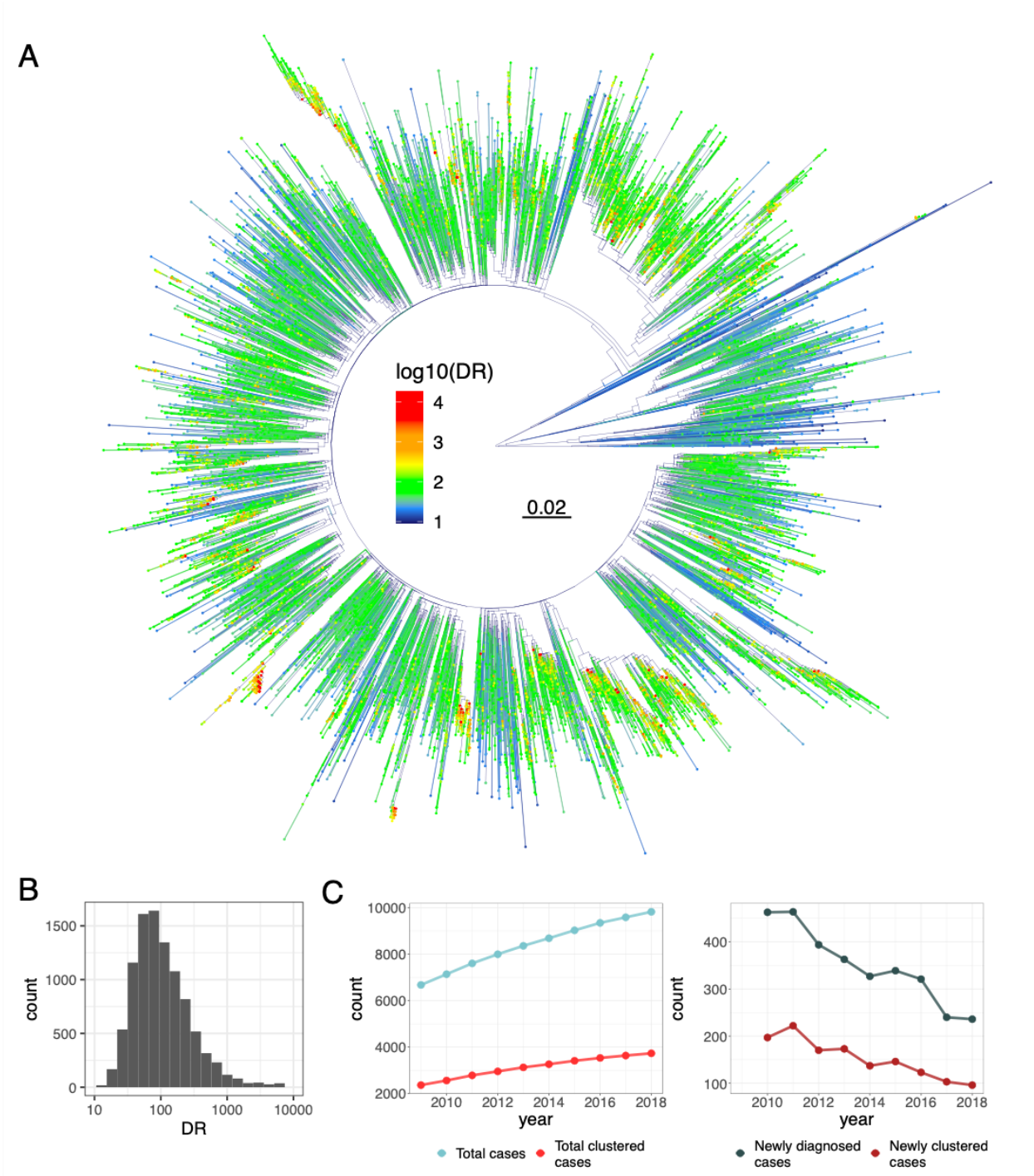

Figure 2.3 Diversification rate distribution, phylogeny and clustering over time. A) 95% majority-rule consensus tree for 2018, with tips and pendant edges colored by lineage-level diversification rate (DR). Warmer colors and thicker edges highlight high diversification rates, suggesting rapid transmission. B) The distribution of lineage-level diversification rates for all individuals. The right-tailed distribution indicates that stratifying by diversification rate is likely to be effective in distinguishing a small top-priority population of individuals. C) Change in total cases, total clustered cases, newly diagnosed cases and newly clustered cases over time. Although total cases and total clustered cases are increasing over time, the yearly numbers of newly diagnosed cases and cases joining clusters have been consistently declining since 2011.

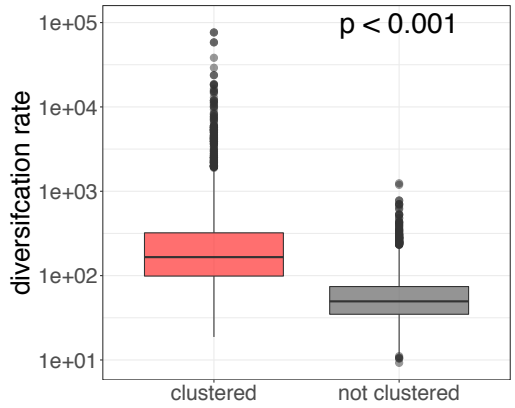

Figure 2.4 Diversification rates in clustered vs. not clustered individuals. Boxplot comparing the median and IQR of the diversification rates from all clustered tips versus all non-clustered tips. Significance of the difference between the two groups was assessed via a Mann-Whitney test. The increased diversification rates within clusters suggest potential for more rapid transmission within these groups, and further justify their position as a public health focus.

2.3.1.2 Non-Phylogenetic vs. Diversification Rate-based Measures

Some non-phylogenetic measures and some diversification rate-based measures were effective in distinguishing priority from non-priority clusters, as labelled by the current BC public health protocol. Using the year 2018 as a representative example, four of the six non-phylogenetic measures tested (Prev3YrGrowth, Prev5YrGrowth, ClustSize and PrevYr5CasePlus) showed a significant difference between priority and non-priority clusters (Mann-Whitney $p = 0.024$, 0.076, 0.0073, 0.017), although none of these four demonstrated clearly defined separation between the two populations of clusters (Figure 2.5B). Using these four measures consistently generates low values for low priority clusters, but values for the high priority clusters frequently form a wide distribution, making the two populations of clusters difficult to distinguish (Figure 2.5B).

In 2018, all six of the diversification rate-based measures (MeanDR, MedianDR, MaxDR, Top3MeanDR, Top5MeanDR, MostRecentDR) tested showed a significant difference

between priority and non-priority clusters (Mann-Whitney p = 0.0033, 0.0016, 0.00086, 0.0019, 0.0011, 0.0016). All tested measures except for the MostRecentDR created two clearly distinct peaks between the two groups of clusters, with the most obvious visual distinction between populations occurring for MeanDR, MaxDR, Top3MeanDR and Top5MeanDR (Figure 2.5A).

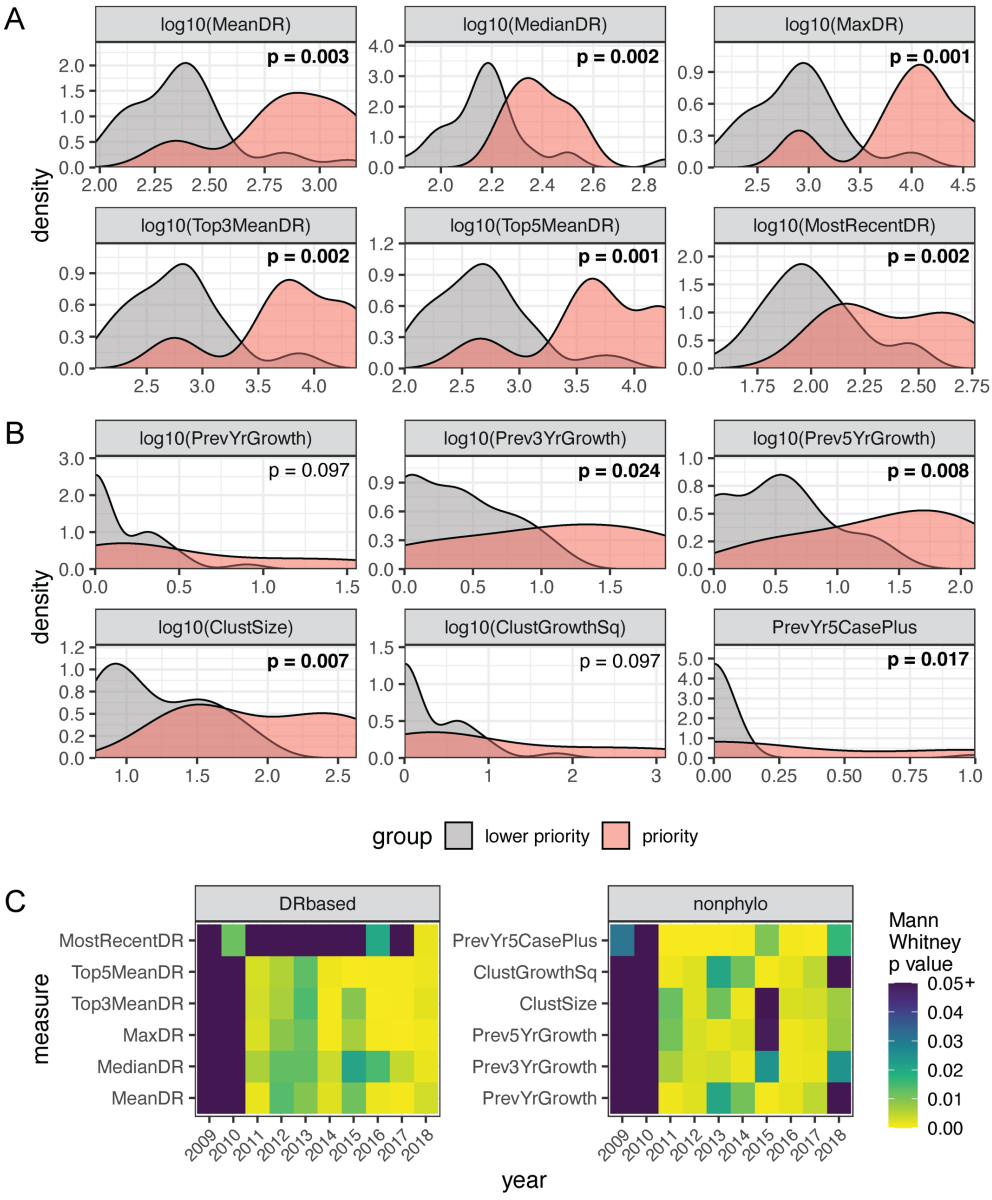

Figure 2.5 Comparison of prioritization measures between priority and non-priority groups, using empirical data. Density plots showing the difference in A) phylogenetic diversification rate-based measures (DRbased) in 2018 or B) non-phylogenetic measures (nonphylo) in 2018 between clusters defined as "priority" by the

current public health protocol for immediate intervention and the remainder of the clusters to next be addressed, marked here for the purpose of comparison as "not priority". Only clusters that had newly diagnoses cases added in the previous year are shown. Infinite values created by the log10 transformation were forced to 0 for visualization purposes. C) Heatmap of significance (as per Mann-Whitney U tests) of the separation between priority and lower priority groups, as produced by the measures we examined. P-values of 0.05 or higher are shown in purple. Rows represent different measures, and columns represent years. Diversification rate-based measures often show greater consistency in their ability to reveal a statistically significant difference between top priority and lower priority clusters across the ten year period investigated than the non-phylogenetic measures.

Assessing the tested measures over a 10-year period illuminated differences in consistency between measures and highlighted need for longitudinal testing of novel prioritization measures. Although many of the measures were relatively consistent over time, none achieved statistical separation in all ten years (Figure 2.5C). The most consistently effective non-phylogenetic measure, PrevYr5CasePlus, creates statistical separation in nine years, but never creates two clearly visually distinct population peaks, possibly due to it's binary nature.

The next most consistent non-phylogenetic measure, Prev3YrGrowth, creates statistical separation in eight years and provides somewhat clearer separation between the populations suggesting that this may be the best non-phylogenetic candidate. However, all diversification rate measures except MostRecentDR offer clearer visual separation between the populations while still achieving statistical separation in eight years, meaning that these measures are at least similarly effective in differentiating the two populations, while potentially offering clearer boundaries.

2.3.2 Simulated data

Phylogenies inferred from simulated data further demonstrated the strength of the relationship between phylogenetic diversification rate-based prioritization measures and future cluster growth, while also revealing differences in this relationship between the two groups of

prioritization measures as the cluster growth period is extended. In general, across parameter sets, the correlation between a prioritization measure and cluster growth in the next year was slightly stronger for the diversification rate-based measures than for the non-phylogenetic measures (median Spearman r = 0.34 vs. 0.29; Figure 2.6). The difference between the two

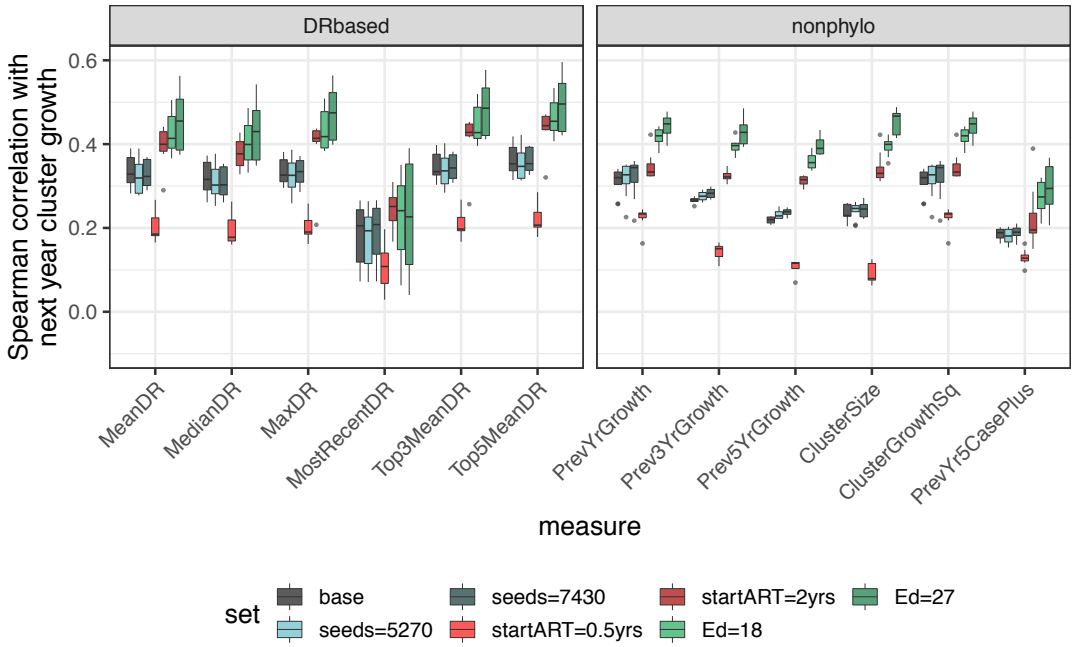

Figure 2.6 Comparison of correlation between prioritization measures and growth in the next year, using simulated data. Each box represents all growth periods from 2009-2018 for a given prioritization measure and parameter set, showing the median and IQR Spearman correlation. The tested parameter sets include variations from the base set that differ in number of seed individuals, time between infection and the initiation of ART (startART) and the expected degree (Ed) of connectedness within the contact network. In general, diversification rate-based measures showed slightly stronger correlations with growth in the next year non-phylogenetic measures.

groups of prioritization measures becomes more striking when considering total future growth of a cluster across the remainder of the simulation period, with the diversification rate-based measures clearly showing stronger correlations across all parameter sets (median Spearman r = 0.39 vs. 0.17; Figure 2.7).

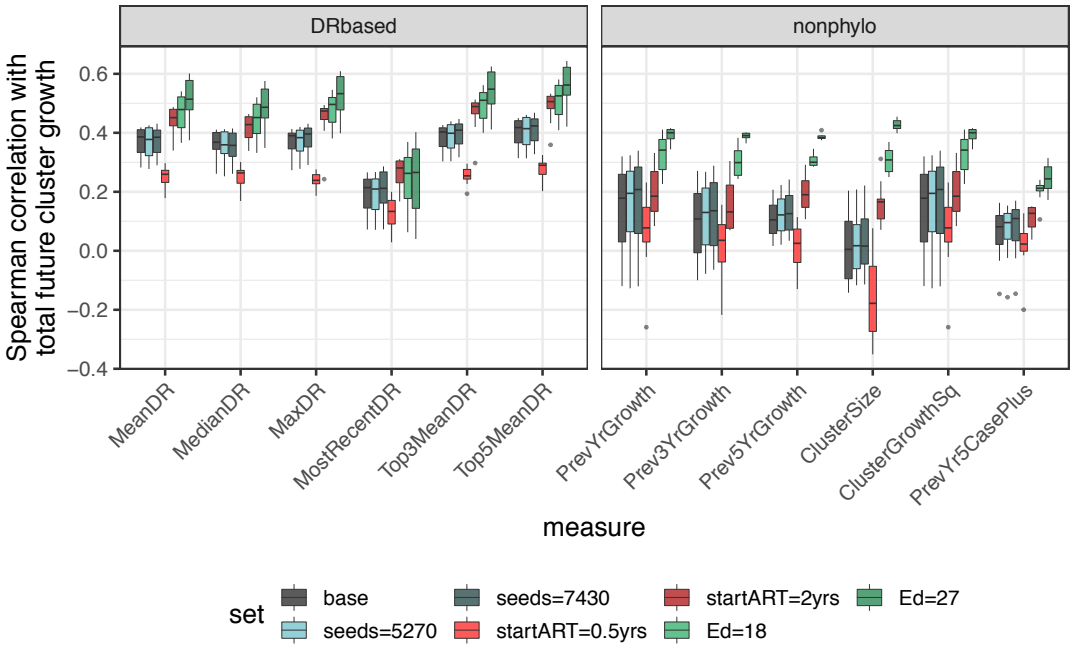

Figure 2.7 Comparison of correlation between prioritization measures and total future growth, using simulated data. Each box represents the median and IQR of the Spearman correlation between a given prioritization measure and parameter set combination and total future cluster growth from each simulation year to the end of the simulation period, across all growth periods from 2009-2018. Parameter set abbreviations are as defined in Figure 2.6. In general, diversification rate-based measures showed stronger correlations with total future cluster growth than non-phylogenetic measures.

Downsampled datasets revealed that as sampling proportion decreases to 75%, 50% and 25%, the positive relationship between diversification rate-based measures and growth in the next year weakens and, in some cases, becomes almost non-existent (median Spearman r = 0.15, 0.08, 0.04), suggesting that these measures are limited in the benefit they can confer in heavily under-sampled epidemics (Figure 2.8). However, the correlation between non-phylogenetic measures and next year growth not only experiences weakening in response to downsampling, but also reversal (median Spearman r = -0.15, -0.21, -0.35; Figure 2.8), meaning that without careful interpretation, non-phylogenetic measures have the potential to become actively misleading in a poorly sampled epidemic.

The relationships with total future growth in the remainder of the simulation period as

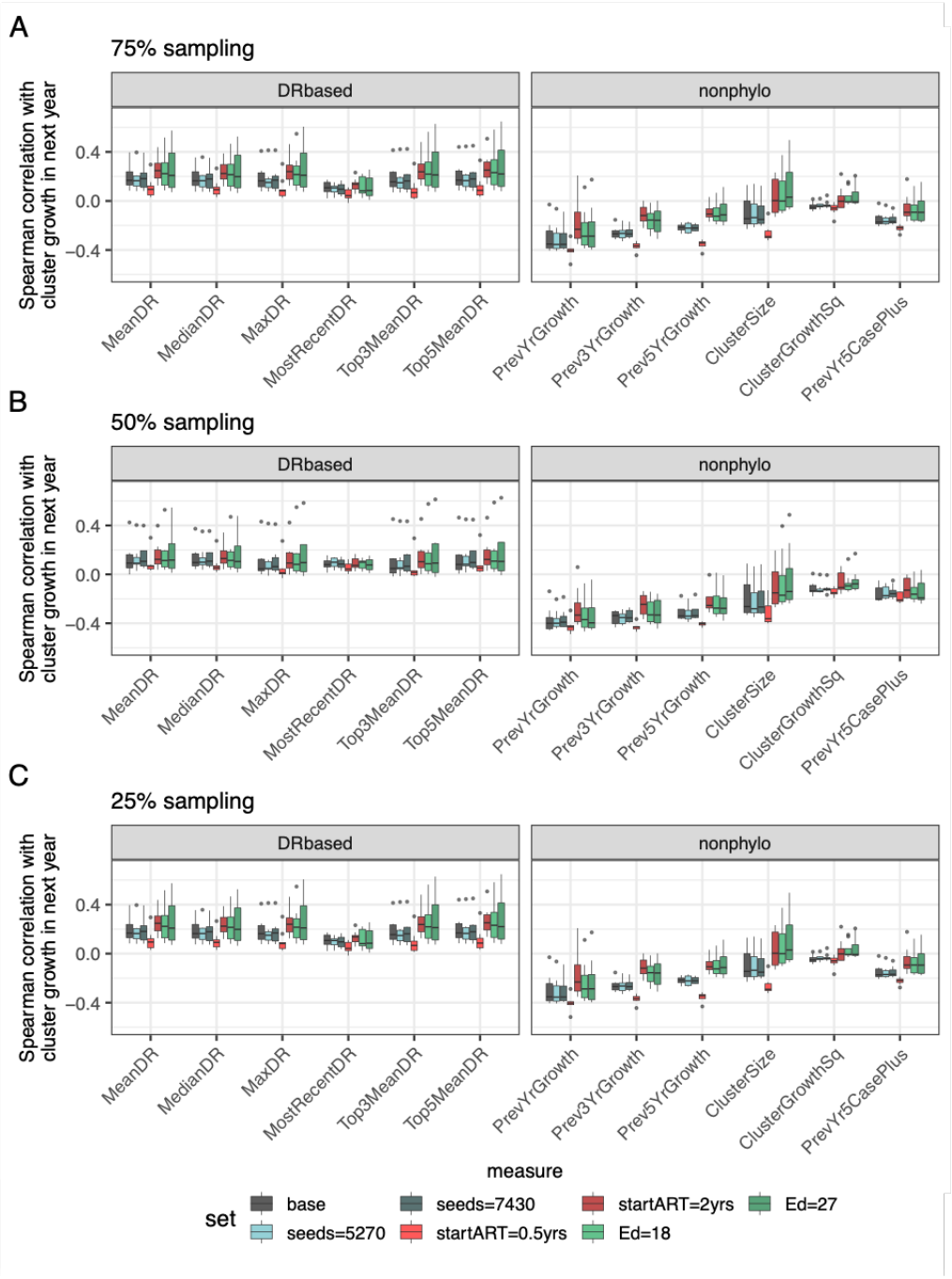

Figure 2.8 Downsampled comparison of correlation between prioritization measures and growth in the next year. Boxplots show the median and IQR of the Spearman correlations between a given prioritization measure and cluster growth in the next year at A) 75% sampling, B) 50% sampling, and C) 25% sampling. Parameter set abbreviations are as defined in Figure 2.6. As sampling proportion decreases, the positive relationship between diversification rate-based measures and growth in the next year weakens and, in some cases, becomes almost non-existent. However, the correlation between non-phylogenetic measures and next year growth not only experiences weakening, but also reversal.

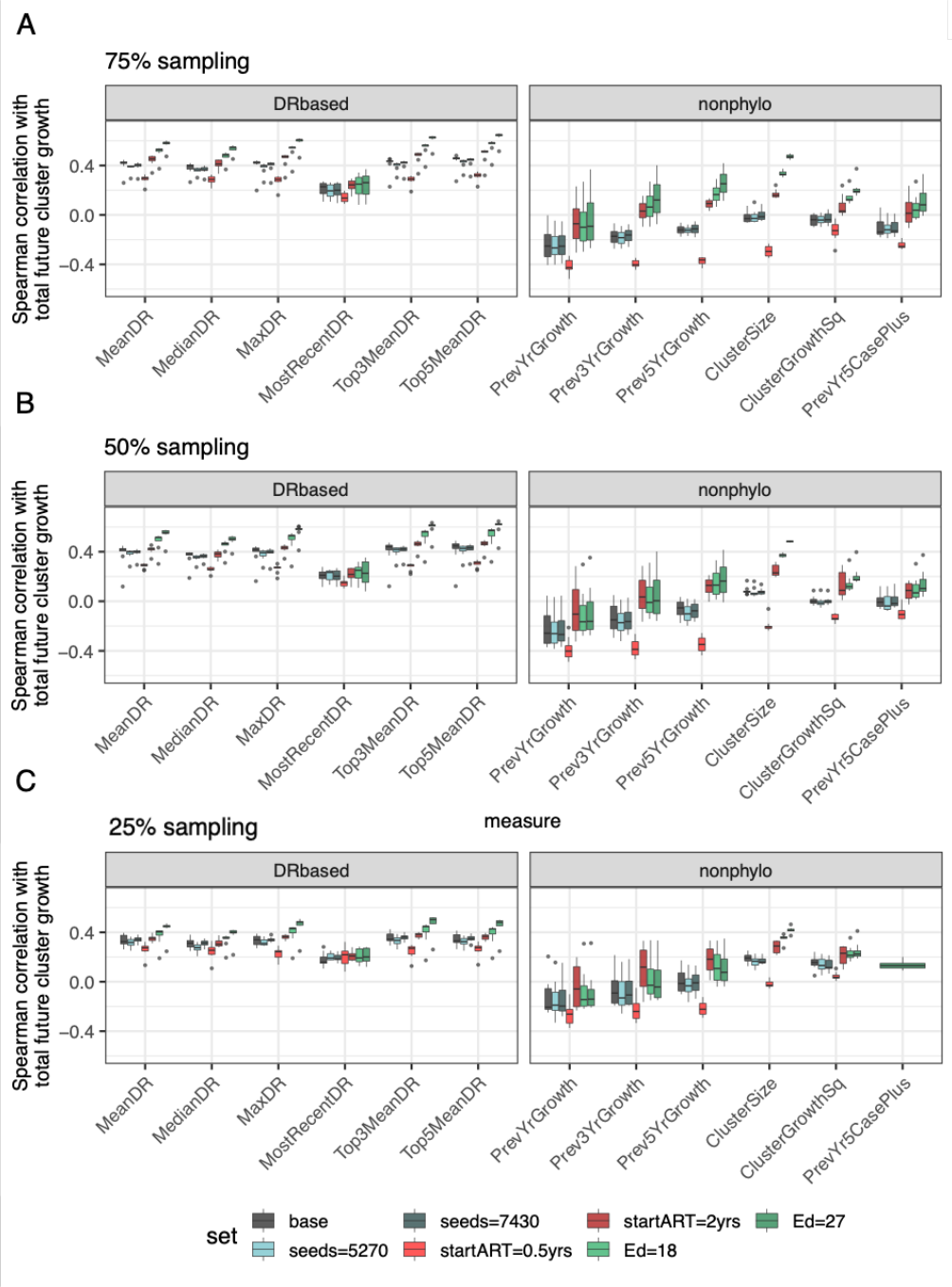

Figure 2.9 Downsampled comparison of correlation between prioritization measures and total future growth. **Boxplot comparing the median and IQR of the Spearman correlations between a given prioritization measures and total future cluster growth at A) 75% sampling, B) 50% sampling and C) 25% sampling. Parameter set abbreviations are as defined in Figure 2.6. Diversification rate-based measures demonstrate very little change in correlation with future growth as sampling proportion is decreased, and although some non-phylogenetic measures such as previous year growth again show inverted correlations, other measures such as cluster size and cluster growth squared retain a relatively similar effect size, particularly when time to start ART or the number of contacts is increased from the base parameter set.**

sampling proportion decreases are more robust for both groups of measures (Figure 2.9). Diversification rate-based measures demonstrate very little change in correlation with future growth as sampling proportion is decreased (median Spearman r = 0.41, 0.40, 0.33), and although some non-phylogenetic measures such as PrevYrGrowth again show inverted correlations, other measures such as ClustSize and ClustGrowthSq retain a relatively similar effect size, particularly when the time to start ART or the number of contacts is increased from the base parameter set (Figure 2.9).

Considering a longer time period of cluster growth also reveals opposing temporal trends in the two groups of measures. Comparing the correlations between prioritization measures and next year growth versus total future growth revealed that effect sizes for diversification rate-based measures strengthened as the length of the cluster growth period was extended, but the opposite trend was seen for non-phylogenetic measures (Figure 2.10), suggesting that diversification rate-based measures may have a stronger relationship with long-term cluster growth. Furthermore, as the starting year for the cluster growth period becomes closer to the present, the strength of correlation for diversification rate measures remains relatively stable, but the strength of correlation for non-phylogenetic measures weakens slightly (Figure 2.10). Downsampled analyses showed that as sampling proportion decreases, the overall relationship between future growth and diversification rate-based measures weakens, but the increasing trend in effect size as the cluster growth period is extended is maintained (Figure 2.11). The weakening of this relationship is notably smaller for the total cluster growth periods than for those including only the next year after prioritization. The relationship between non-phylogenetic measures and future growth also weakens as sampling proportion decreases, but with the greatest decrease occurring for the next-year periods, such that the previous trend of weakening

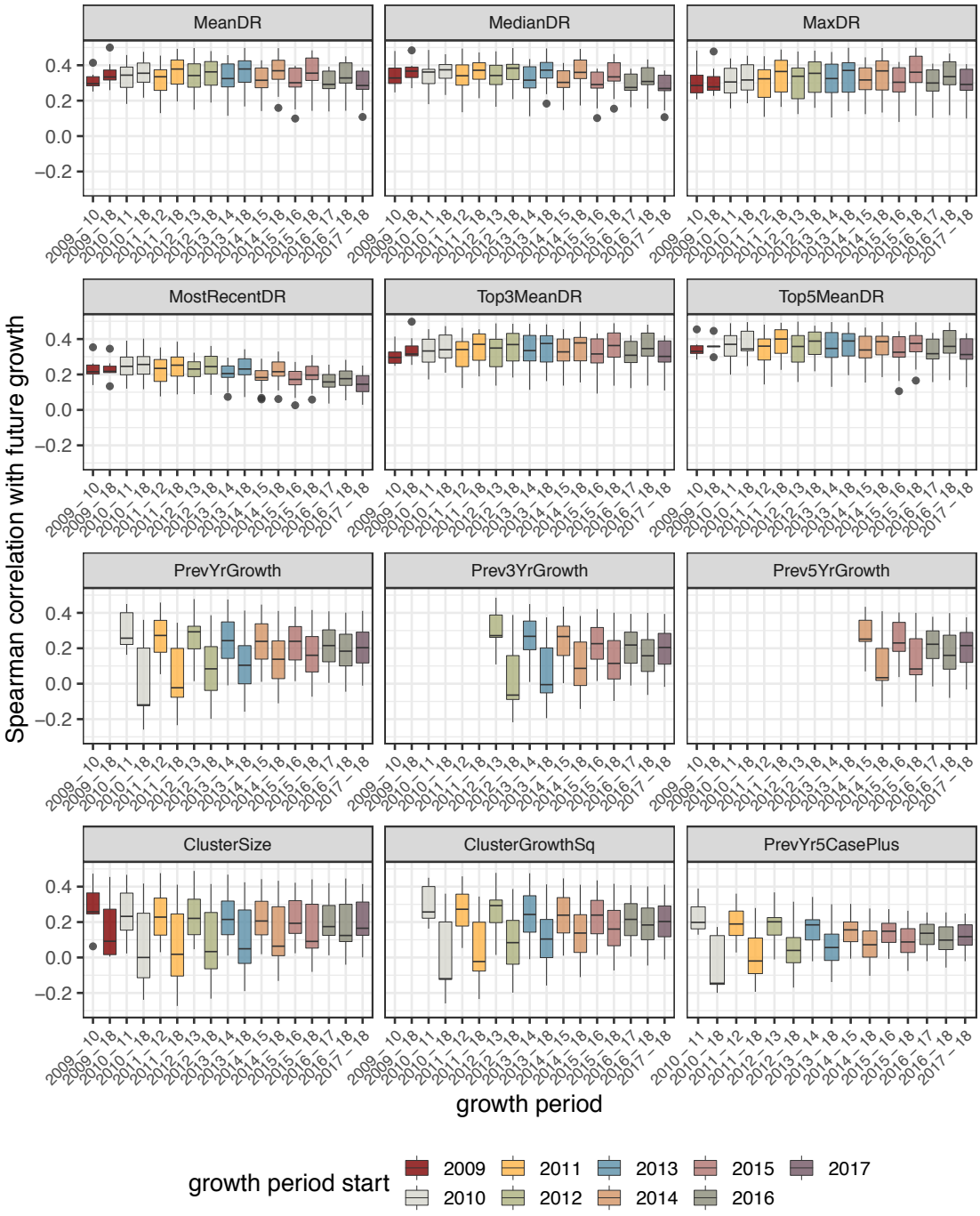

Figure 2.10 Spearman correlation between each prioritization measure and cluster growth over time. Growth periods end either in the year following prioritization measure calculation or the final year of the simulation (anywhere from one to nine years after prioritization, depending on the starting year). Boxes show the median and IQR of the effect sizes for each growth period, across all parameter sets. Boxes are colored based on the starting year of the growth period, ie. the year of prioritization. Diversification rate measures showed a small increase in effect size as the growth period was extended from the next year to the full simulation period, but the opposite trend was seen for non-phylogenetic measures.

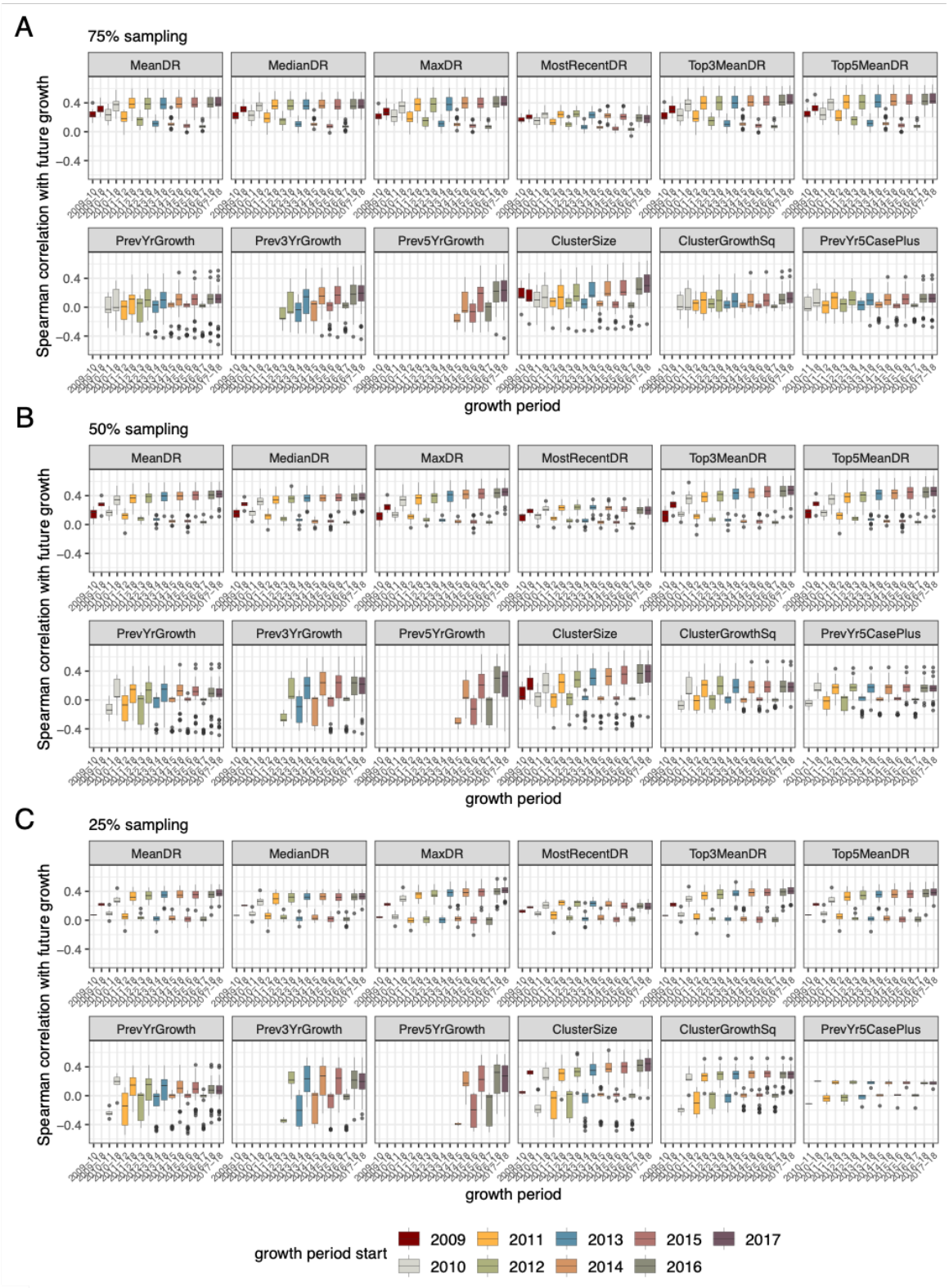

Figure 2.11 Downsampled Spearman correlation between each prioritization measure and cluster growth over time. Mean Spearman correlation between each prioritization measure with future cluster growth,

sampled at A) 75%, B) 50% and C) 25%. Growth periods end either in the year following prioritization measure calculation or the final year of the simulation (anywhere from one to nine years after prioritization, depending on the starting year). Boxes show the median and IQR of the effect sizes for each growth period, across all parameter sets. Boxes are colored based on the starting year of the growth period, ie. the year of prioritization.

correlations as the growth period extends is reversed. As observed with diversification rate measures, the relationship between future growth and non-phylogenetic measures was also most robust to decreasing sampling proportion when considering total future growth (Figure 2.11).

Differences in the relationship between prioritization measures and future growth also exist across parameter sets. Regardless of growth period, both diversification rate and non-phylogenetic measures show much weaker correlations with cluster growth when the time to start ART is reduced to 0.5 years (Figure 2.6, 2.7). Conversely, as the time to start ART is increased to two years, correlations strengthen, even relative to the base parameter set. This trend continues even further when the average level of connectedness of individuals within the contact network increases. Additionally, when the time to start ART is increased or the expected degree of connectivity is increased, correlations with total future growth are more robust to downsampling. Together, these results suggest that prioritization measures as a whole may be at their most useful in epidemics with longer delays in connection to care, more connected at-risk populations and more barriers to treatment and prevention.

Analysis of the difference between the number of transmissions resulting from top-ranking prioritized clusters and a random sample of lower-ranking clusters containing the same number of individuals demonstrated additional benefits of using diversification rate-based measures. Without adjusting for cluster size, the difference in direct transmissions stemming from prioritized versus not prioritized clusters was higher for non-phylogenetic measures for all parameter sets (except when time to start ART is 0.5 years). However, when the number of direct

transmissions was adjusted for current cluster size, diversification rate-based measures showed larger differences in direct transmissions (Mann-Whitney $p < 0.001$) in the majority of parameter sets, with a notably larger disparity for parameter sets with increased time to start ART or contact network connections (Figure 2.12). The shift in outcome after adjusting for cluster size perhaps suggests that diversification rate-based measures are more likely to prioritize smaller

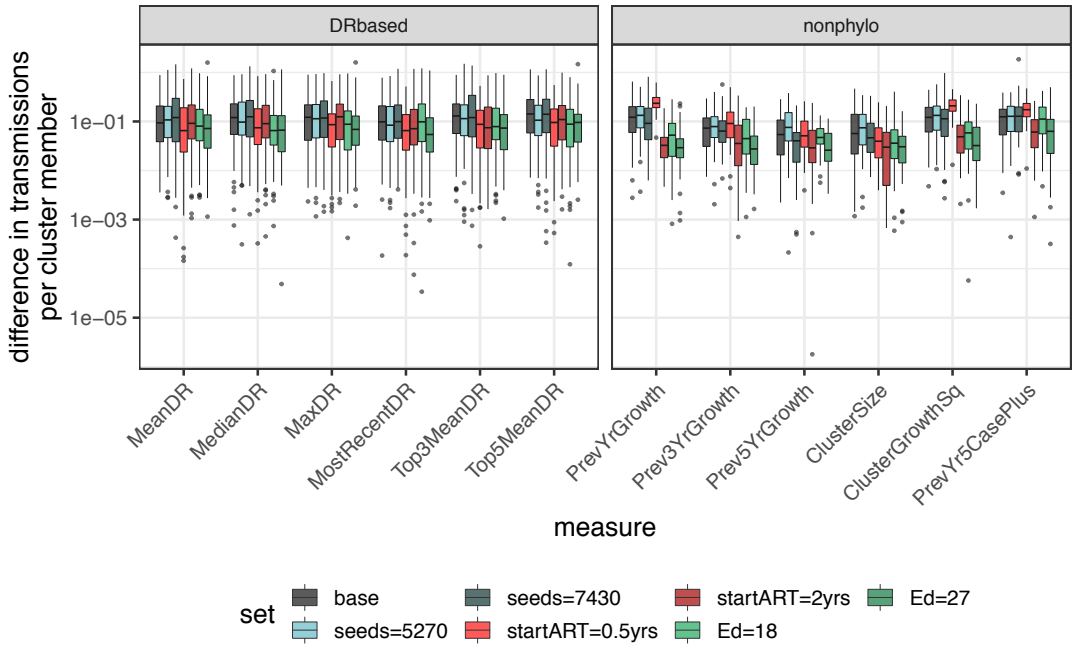

Figure 2.12 Difference in downstream transmissions across all prioritization measure and parameter set combinations. Each box represents the median and IQR of the difference in mean direct transmissions per cluster member between the top prioritized clusters, up to inclusion of 100 individuals (or the size of the top cluster, if its size exceeds 100), according to a given prioritization measure and a random sample of lower-ranking clusters containing the same number of individuals, across all clusters. The difference in mean direct transmissions was, in general, slightly higher for diversification rate-based measures than for non-phylogenetic measures, with the exception of previous year cluster growth in some parameter sets. Parameter set abbreviations are as defined in Figure 2.6.

transmission clusters, capturing individuals with potential for rapid transmission that may otherwise go undetected until the cluster undergoes an amount of growth large enough to result in non-phylogenetic prioritization. Indeed, median cluster sizes were significantly smaller (Mann-Whitney $p < 0.001$) for clusters prioritized by diversification rate measures (median size

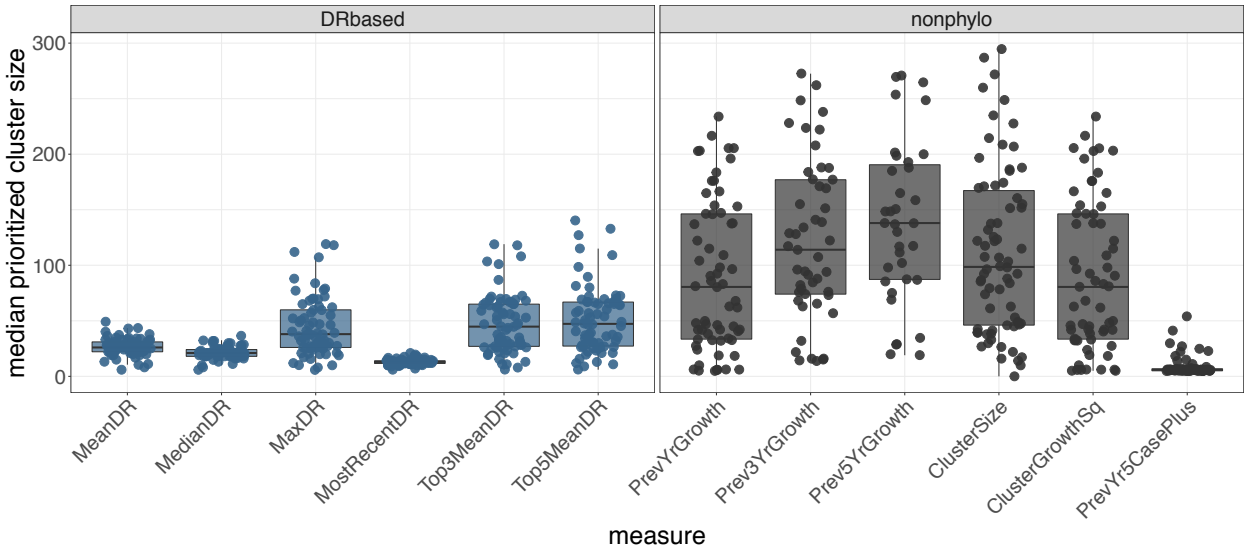

Figure 2.13 Comparison of prioritized cluster size across prioritization measures. Boxplot comparing the median and IQR of the median size of the clusters prioritized by each prioritization measure. In most cases, median cluster sizes are smaller for clusters prioritized by diversification rate measures than for clusters prioritized by non-phylogenetic measures.

= 41) than for clusters prioritized by non-phylogenetic measures (median size = 99; Figure 2.13), with the exception of PrevYr5CasePlus, which is biased by the fact that cluster initiation begins with a jump in size from zero to five. Diversification rate measures also showed greater consistency across parameter sets, indicating their ability to retain relevance in a wider range of scenarios. Downsampling demonstrated a similar trend to that of previous analyses, showing that decreases in sampling proportion generally result in maintenance of difference in transmissions for diversification rate measures (with the exception of one parameter set at 25% sampling) while the non-phylogenetic measures undergo a decline (median difference in transmissions = 0.16, 0.16, 0.13 vs. 0.13, 0.12, 0.08; Figure 2.14).

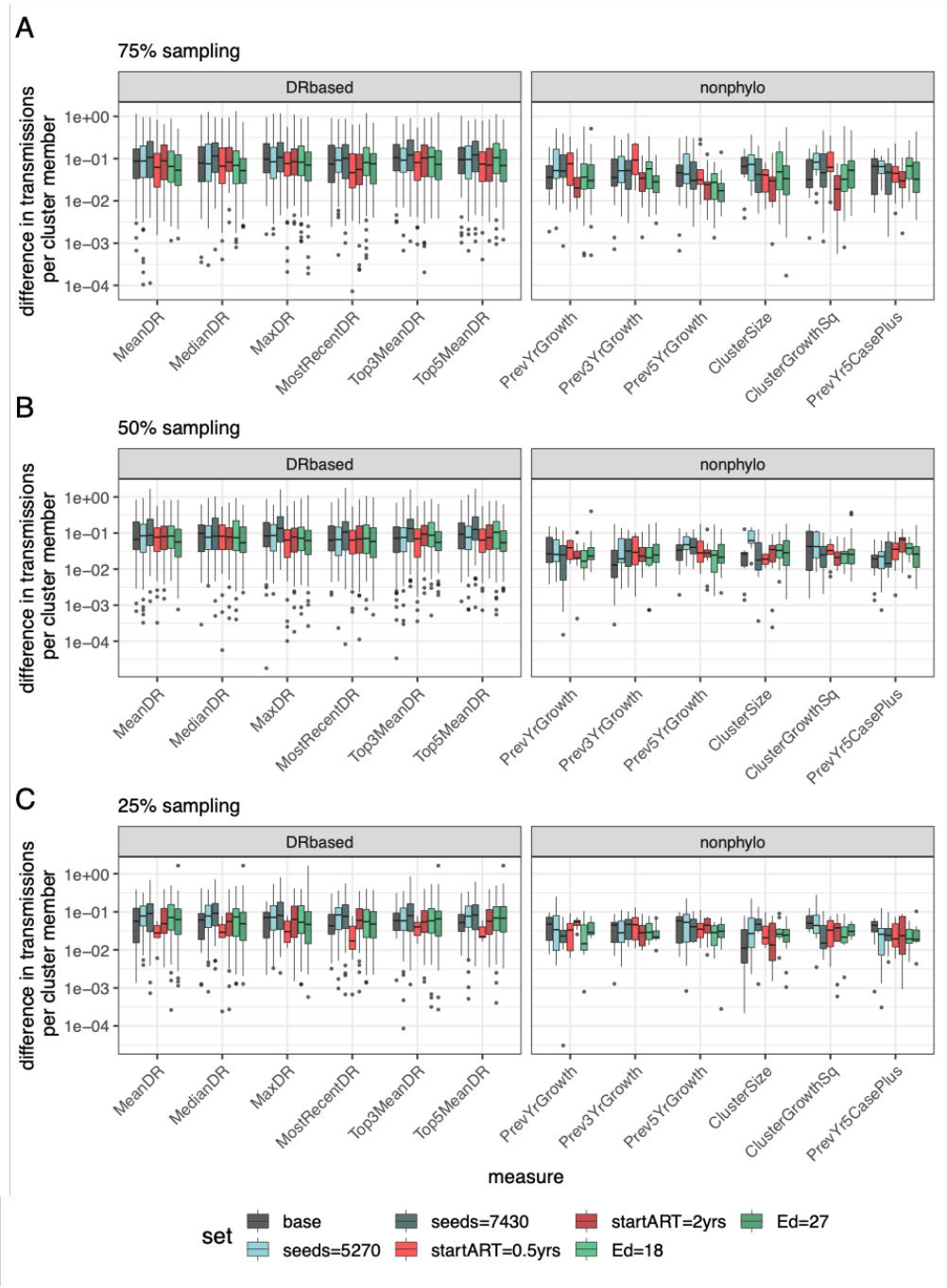

Figure 2.14 Downsampled difference in direct downstream transmissions across all prioritization measure and parameter set combinations. Boxplot comparing the median and IQR of the difference in mean direct transmissions per cluster member between the top prioritized clusters, up to inclusion of 100 individuals, according to a given prioritization measure and a random sample of lower-ranking clusters containing the same number of individuals, at A) 75% sampling, B) 50% sampling and C) 25% sampling. Parameter set abbreviations are as defined in Figure 2.6. in sampling proportion generally result in maintenance of

difference in transmissions for diversification rate measures (with the exception of one parameter set at 25% sampling) while the non-phylogenetic measures undergo a decline.

2.4 Discussion

This study revealed differences in the effectiveness of multiple lineage-level diversification rate-based and non-phylogenetic prioritization measures in identifying potential for future transmission, via both empirical and simulated data approaches. Phylogenetic clustering of viral sequences provides a platform for prioritization of groups that aims to maximize the benefits of limited public health resources while still maintaining patient confidentiality. However, existing methods of prioritization are limited by their subjectivity and reliance on historical or linked data. Previous studies have demonstrated the advantages of prioritizing transmission clusters based on non-phylogenetic measures such as the square of cluster growth[37] and phylogenetic measures such as the terminal branch length[40]. In concordance with Moshiri *et al*. (2021)[40], we find phylogenetically derived measures, specifically those derived from lineage-level diversification rates, confer several advantages.

In the empirical BC dataset, measures based on phylogenetically derived lineage-level diversification rates demonstrated relatively similar ability to delineate prioritized clusters from less urgent clusters relative to non-phylogenetic measures overall. Simulated data further supported this, revealing a stronger relationship between the large majority of diversification rate-based measures and future cluster growth than seen for non-phylogenetic measures. The disparity in the strength of this relationship between diversification rate and non-phylogenetic measures becomes greater when the growth period under study is extended from only the next year to all future years remaining in the simulation period, suggesting that diversification rate-based measures are more closely associated with long-term growth. This confers an additional

advantage to diversification rate-based measures, as a strong relationship with long-term growth could further maximize the downstream benefit of the public health resources distributed following prioritization. However, diversification rates may be limited in that they are responsive to branch length differences that may result from differences in cluster transmission rates or sampling rates, rather than directly measuring individual or cluster characteristics that drive differences in transmission. Despite this, diversification rates remain useful in that they are reflective of historical transmission dynamics associated with individuals. Other work has shown that similar phylogenetic measures capture sexual contact network features in the absence of any direct information about the network[40], indicating that some detection of non-phylogenetic factors linked to potential for transmission is possible without direct measurement. Analyses of decreased sampling proportion revealed further advantages of diversification rate-based measures, which were more consistently robust to the effects of missing data than non-phylogenetic measures. The practical implications of this finding are important as even the most well-sampled epidemics rarely come close to 100% sampling, so in order to be widely applicable, a prioritization measure needs to be robust to the effects of missing data in a wide range of epidemic circumstances. However, it should be noted that random downsampling will not provide an exact recapitulation of natural sampling bias, and the true effects of lower sampling proportion may differ from our findings. Another potential advantage of diversification rate measures is that in the case of larger clusters, they could be used to reveal subpopulations within a cluster in need of rapid intervention, even in cases where the cluster as a whole may not be prioritized.

Both empirical and simulated data revealed similar trends in the overall abilities of individual measures. Measures based on the most recent diversification rate(s) consistently

performed considerably worse relative to other measures, further demonstrating the limited abilities of measures failing to capture long-term trends. In contrast, MaxDR, MeanDR, Top3MeanDR and Top5MeanDR offered the most consistency, achieving statistically significant separation between the urgent priority and remaining population of clusters in eight of the years studied. Although two non-phylogenetic measures (PrevYr5CasePlus, Prev3YrGrowth) meet this standard, they rely entirely on the existence of historical data, a shortcoming that could be eliminated by use of diversification rate-based measures. One such measure, Top5MeanDR, not only achieves statistically significant separation in eight of the ten years studied in the BC dataset, but also shows the strongest relationship with cluster growth across all simulated growth periods and parameter sets studied of all tested prioritization measures. This is in concordance with analyses conducted by McLaughlin *et al*. in 2019[44], which find the mean of the top five log diversification rates in a geographic area to be a significant predictor of new HIV cases in BC. However, several other measures displayed consistent ability to delineate clusters based on priority status in addition to showing relatively strong relationships with future cluster growth, and as suggested by McLaughlin *et al*., it is likely that prioritization could be further optimized beyond the reaches of a single measure via a model combining multiple factors[44,45]. Furthermore, as mentioned by Moshiri *et al.*[40], even a combined measure is unlikely to capture the full context of the epidemic, and measures that aim to improve the prioritization process should still be considered in the context of other supporting knowledge.

2.5 Conclusions

Overall, we find that diversification rate-based measures not only frequently outperform non-phylogenetic measures in their ability to identify groups with the highest potential for future

growth, particularly long-term future growth, but are also less likely to be perturbed by missing data and remain free of need for historical data and subjective interpretation. In contrast, although non-phylogenetic measures can sometimes be equally effective as measures based on phylogenetic diversification rates, they have the potential to become misleading in cases of lower sampling proportion. In combination with phylogenetic clustering, phylogenetically-derived lineage-level diversification rates can provide a simple, widely applicable and robust solution to focus prioritization of transmission clusters contributing the most to an ongoing epidemic.

Chapter 3: Expansion of HIV transmission clusters among key populations in association with SARS-CoV-2 lockdown

3.1 Introduction

As transmission of SARS-CoV-2 became a global public health crisis in early 2020, the initial defense strategy chosen by many regions was to recommend and implement restrictions designed to drastically reduce levels of connectivity within and between communities. In order to interrupt transmission chains quickly and curtail exponential spread, restrictions are often constructed with broad application in mind and can have unintended consequences[52]. Broad restrictions have been shown to disproportionately affect vulnerable subpopulations who rely on social, economic and medical supports, the disruption of which can further exacerbate challenges such as food insecurity[53,54], gender-based violence[55,56], management of medical conditions[57,58] and drug use[59,60]. The population of individuals living with or at-risk of HIV infection is also vulnerable to such impacts, as the successful management and prevention of HIV often requires access to clinics and services that may be shut down or limited in capacity as a result of COVID-19 restrictions. Without access, individuals may be left without diagnostic testing, viral load testing, ART, pre-exposure prophylaxis (PrEP), safe injection materials, condoms and other resources crucial to keeping pathogen transmission controlled within at-risk communities. Reduced engagement with and availability of HIV treatment and prevention services in association with COVID-19 and its related restrictions has been documented in many countries[60-67], in some cases coinciding with worsening HIV outcomes such as viral load rebound[66] or progression to AIDS[65]. Even in locations such as Australia with very few early interruptions to HIV care[68], both HIV

tests[69] and PrEP use[70] reportedly decreased, perhaps due to reduced risk behaviours or hesitancy to risk COVID-19 infection by visiting a hospital or clinic. The effects of the COVID-19 pandemic on HIV care and epidemic control present a complicated challenge to global public health systems, and quantification of the downstream effects of this disruption is necessary for design of effective countervailing strategies.

In the province of BC, Canada, several different types of restrictions amounting to the region's first "lockdown" were announced during March 2020[71], culminating on March 21st (Figure 3.1A). On March 16th, health officials banned gatherings of more than 50 people and ordered bars and nightclubs to close. On March 17th, public schools were ordered to close and the province declared a public health emergency. March 20th saw the closure of dine-in establishments and playgrounds, and personal service establishments were shut on March 21st. Although no official work-from-home order was put in place, many employers shifted their employees out of the office during mid-March, further contributing to reduced contact rates. During this time, many sites offering health-related services reduced their capacity and hours of operation. Even essential services that were encouraged to stay open, such as safe injection sites, underwent notable declines in availability as the necessary adaptations to reduce the chance of SARS-CoV-2 transmission were put in place. After approximately two months of lockdown, the reopening of shops, restaurants and public spaces was announced on May 19th, and public schools reopened June 1st. By June 24th, BC was entering the third phase of its reopening plan, marking the beginning of an approximately three-month period with minimal restrictions before the "second wave" of transmission began in October 2020.

A potential positive side effect of the restrictions enacted in BC being followed by a dramatic increase in amount of time spent at home is that for some populations at risk of HIV

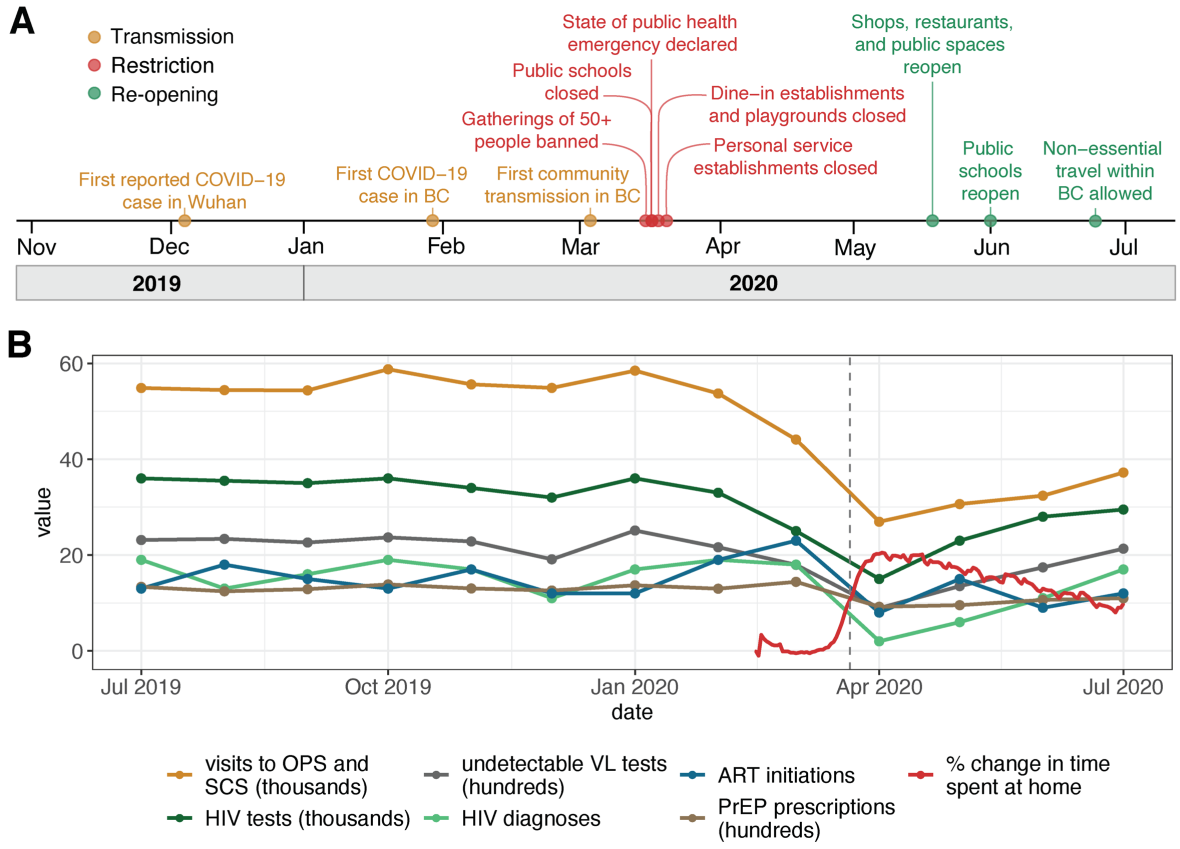

Figure 3.1 Timeline of COVID-19-related events in British Columbia. The majority of restrictions were put in place during mid-March, 2020, culminating on March 21st. (B) Reduction in engagement with HIV prevention and management services following the implementation of lockdown restrictions coincides with increases in the amount of change to time spent in residential locations. The grey dashed line marks March 21st. Abbreviated markers of engagement include viral load (VL) tests yielding undetectable viral load, pre-exposure prophylaxis (PrEP) prescriptions, antiretroviral therapy (ART) initiations, and visits to overdose prevention services (OPS) and safe consumption sites (SCS). Change in time spent at home was assessed using the Google COVID-19 Mobility Reports data. Data describing monthly engagement with HIV prevention and management services were collected by the BC-CfE Drug Treatment Program and the BC Centre for Disease Control (BCCDC). Data describing visits to OPS and SCS originated from the BCCDC Overdose Response Indicator Report.

infection, contact rates were likely reduced, thus reducing the chance of transmission. This phenomenon has been documented in MSM in Australia[72] and the UK[73], where reductions in number of sexual partners were reported in association with COVID-19 awareness and restrictions. In BC, a study of sexual health service clients found that 31% reported a reduction in partners during the pandemic[74]. However, populations characterized by non-sexual transmission

routes such as shared needles may have experienced increased transmission risk as facilities such as safe injection sites reduced capacities whilst drug use[60,75], overdose calls[76,77] and risky transactional sex[78] increased, possibly due to pandemic-related stressors[79,80] and increased financial instability[78]. Pandemic-related disruptions to health services have also been shown to contribute to increases in HCV transmission[81] which is primarily transmitted by PWID[82]. Additionally, willingness to seek sexual health services may have decreased, as described in a BC study where 66% of participants reported avoiding or delaying interaction with sexual health services during the pandemic[74]. Consequently, we hypothesize that following the initial implementation of lockdown restrictions and reduced access to HIV management and prevention services in BC, key populations of individuals at increased risk for HIV acquisition will demonstrate differential trends in rates of transmission, some of which may not be outweighed by the effects of reduced contact rates. We therefore undertook a series of phylogenetic analyses to quantitatively approximate transmission preceding, during and following the implementations of restrictions.

3.2 Methods

3.2.1 Supporting data and statistical analyses

Data describing monthly engagement with HIV prevention and management services were collected by the BC-CfE Drug Treatment Program and the BC Centre for Disease Control (BCCDC). Data describing visits to Overdose Prevention Services (OPS) and Safe Consumption Sites (SCS) originated from the BCCDC Overdose Response Indicator Report[83]. Movement trends were assessed using the Google COVID-19 Mobility Reports data[84]. Pandemic-related events used in the timeline seen in Figure 1A were selected from a similar timeline published by

CTV News[71]. Mann-Whitney tests quantified changes in service engagement from monthly data spanning August 2019 to March 2020 versus April to July, 2020. The relationship between cluster growth and cluster risk factor composition was quantified via Spearman correlation. All statistical analyses were performed in version 3.6.1 of the R statistical framework[85]. R packages used include ape, cowplot, ggtree, lubridate, phangorn, phylobase, phytools, tidyverse, reshape2 and scales.

3.2.2 Phylogenetic analyses

38,408 partial *pol* HIV-1 sequences were collected from 10,386 individuals during drug-resistance genotyping tests performed by the BC-CfE as part of routine clinical care following diagnosis between May 30th, 1996 and June 4th, 2021. The full sequence dataset was aligned with MAFFT[47] and filtered to contain only the earliest sequence per individual, in order to focus phylogenetic inference on between-host evolution. Surveillance drug resistance mutations were masked before maximum likelihood inference of 100 bootstrap phylogenies in IQ-TREE[86] under a GTR+F+R10 model, as determined with ModelFinder[87]. Transmission clusters were determined using a minimum size threshold of five, a 90% bootstrap threshold and a phylogenetic distance threshold of 0.02 substitutions/site, as defined by Poon *et al.*[18]. Cluster growth, branching events and diversification rates were assessed in three sixty-day time periods, including "pre-lockdown" (January 22 – March 21, 2020), "lockdown" (March 22 – May 20, 2020) and "post-lockdown" (May 21 – July 19, 2020).

Adjusted cluster growth was calculated as the number of new cases in a cluster, normalized by cluster size and total new diagnoses during a given time period. Total adjusted

cluster growth was determined by summing the adjusted cluster growth of clusters classified as MSM or PWID.

Daily median branching events, tree bifurcations that suggest transmission, were determined from the ten most likely of 100 bootstraps inferred from alignments excluding all sequences predating 2017, done to increase the precision of time-scaling in LSD2[51]. Rooting in LSD2 was done on all branches using constraints and single variance on branch lengths. Adjusted branching events were calculated as the daily median number of branching events across bootstraps, normalized by size of the linked cluster and total diagnoses in a given time period. The adjusted sum of daily median branching events was calculated by totaling the median number of daily branching events inferred to be associated with clusters classified as each risk factor, normalized by cluster size and new diagnoses during a given time period.

In order to approximate transmission rate, lineage-level diversification rates were calculated as in Jetz *et al*.[42] for each phylogenetic tip in the ten most likely bootstraps and median tip-level change in diversification rate between time periods was summarized by cluster. Changes in lineage-level diversification rates were used to approximate increases in transmission rather than raw diversification rate because diversification rate is expected to increase over time as the likelihood of new sequences being in close phylogenetic proximity to existing sequences rises with increased sampling. Thus, it is more appropriate to compare the magnitude of increase rather than the raw value when making comparisons across time. The ten highest likelihood trees were pruned into four subtrees, representing the beginning, end and time-period divisions within the total time range studied. Diversification rates were calculated for all tips in all subtrees, such that change in median diversification rate across bootstraps for an individual's virus between time periods could be determined. Then, clusters were summarized by determining the median

change in diversification rate across cluster tips in each time period and normalizing by cluster size and time period diagnoses. Total adjusted median change in diversification rate was determined by summing the adjusted median change in diversification rate associated with clusters classified as being associated with each risk factor.

Cluster risk composition was calculated as the proportion of PWID minus the proportion of MSM individuals in a cluster, such that a risk composition of 1 indicates 100% PWID reporting with no reporting of MSM and a risk composition of -1 suggests the opposite. Members of the same cluster may report different risk factors, and a single individual may report multiple risk factors, meaning that some clusters contain substantial risk factor overlap. Stratifying clusters by risk composition allows analysis of trends across the distribution of risk-factor homogeneity and facilitates exclusion of ambiguous clusters when necessary. The University of British Columbia – Providence Health Care Research Ethics Board granted ethical approval for this study (H17-01812).

3.2.3 Risk factor classification

The proportions of individuals reporting different risk factors in a cluster were calculated using data collected after 2016, in order to appropriately represent current trends in transmission for each cluster. In order to capture the branching events more likely to be associated with individuals with a certain risk factor, each event was assigned the risk factor composition of the cluster its descendants were members of. Because clusters are often not entirely homogenous in terms of reported risk factors, this means some branching events will have some descendants reporting risk factors that differ from the overall risk factor classification of the event. There were no cases of descendants being split between multiple clusters, although some descendant

groups contained non-clustered sequences in addition to clustered sequences. In analyses that sum cluster outcomes, binary classification of cluster risk factors was done by labelling all clusters with a cluster risk composition of -0.5 or less as MSM and all clusters with a cluster risk composition of 0.5 or more as PWID. Ambiguous clusters in between these thresholds were not included.

3.3 Results

3.3.1 Reduction in HIV service engagement following lockdown

Individual movement data revealed that following the lockdown restriction announcements culminating on March 21st, time spent at home increased markedly, likely leading to reduced contact rates (Figure 3.1B). Also in April, there were statistically significant reductions in markers of engagement with HIV services, including ART initiation (Mann-Whitney $p = 0.030$), PrEP prescription dispensations (Mann-Whitney $p = 0.00026$), undetectable plasma viral load tests (Mann-Whitney $p = 0.0037$), HIV tests (Mann-Whitney $p = 0.0057$), new HIV diagnoses (Mann-Whitney $p = 0.049$) and visits to Overdose Prevention Services (OPS) and Safe Consumption Sites (SCS) (Mann-Whitney $p = 0.00017$) (Figure 3.1B). Importantly, as the lockdown period began, the BC-CfE recommended reduction in viral load testing frequency in patients with long-term viral load suppression, in order to preserve SARS-CoV-2 testing capacity. This directive is likely responsible for at least some of the reduction in undetectable viral load tests. Post-lockdown, all markers of engagement rebounded to below pre-lockdown levels. New HIV diagnoses in the province remained on an overall declining course.

3.3.2 Transmission changes following lockdown

New diagnoses decreased from 44 during the pre-lockdown period to 18 during lockdown and began to rebound thereafter (26 post-lockdown). As suggested by the dip in service engagement during lockdown, it is likely that sampling proportion of newly diagnosed infections also declined during this time, meaning that the decrease in diagnoses does not necessarily indicate a proportional decrease in transmission. Further phylogenetic analyses support this idea and suggest that the magnitude of transmission occurring differs between risk groups.

When normalized by cluster size and total number of new diagnoses in each month, cluster growth demonstrated a peak in the strength of its relationship with cluster risk factor proportion during the lockdown period (Figure 3.2A). Although not significant, the pre-lockdown and post-lockdown periods show negative correlations between adjusted cluster growth and cluster risk composition (Spearman $r = -0.044, -0.21$; $p = 0.87, 0.55$), while a strong positive correlation exists during the lockdown period (Spearman $r = 0.8$, $p = 0.13$), indicating higher growth as cluster risk composition shifts towards 100% PWID. Furthermore, a strong positive correlation is not seen in any of the three equivalent time periods during the previous three years (Figure 3.3). Analyses of both total and median adjusted cluster growth reveal that MSM-dominant clusters experience a notable decline to near zero during lockdown, while PWID populations peak at a level unseen during any of the equivalent time periods in the previous three years (Figure 3.2B, 3.4).

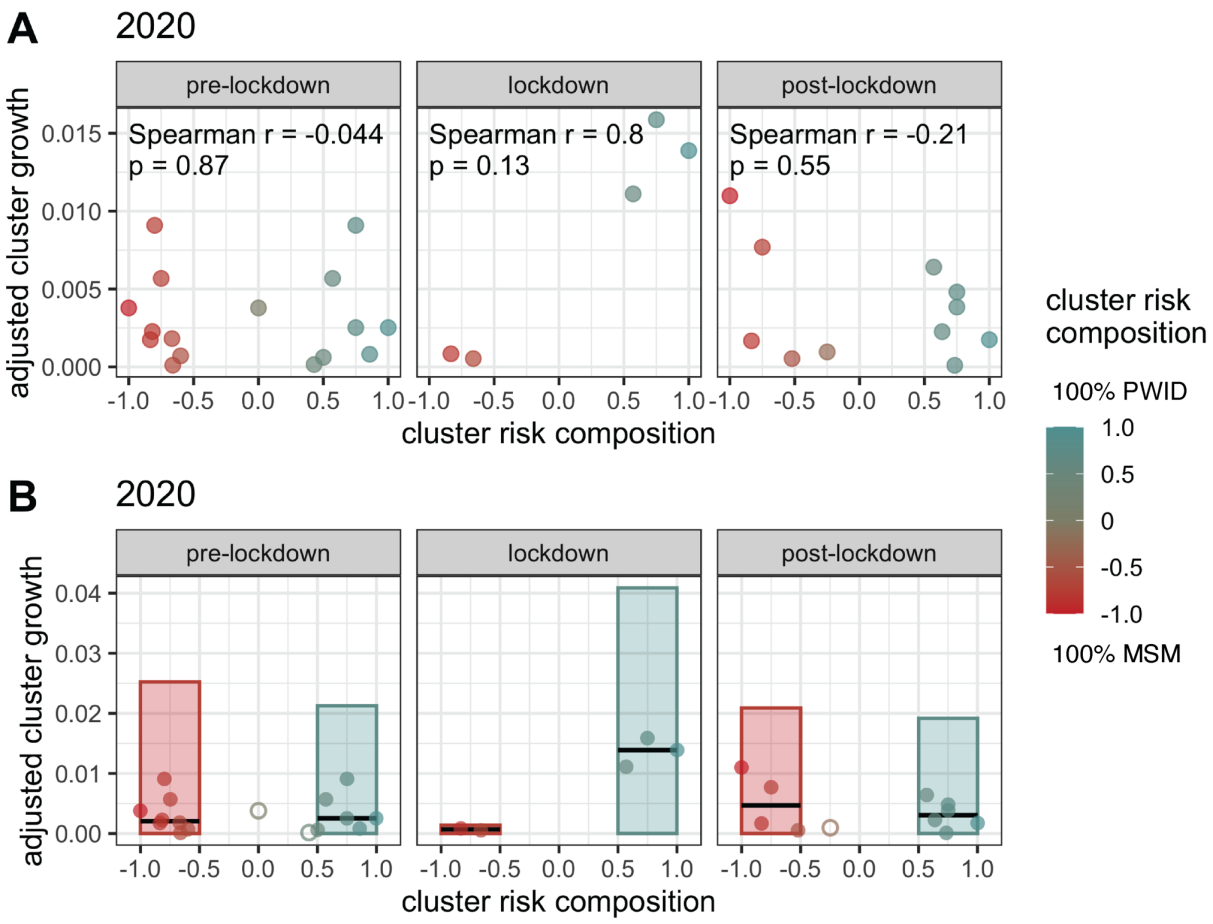

Figure 3.2 Differences in adjusted cluster growth by risk factor composition. A) Adjusted cluster growth versus cluster risk composition, defined as the proportion of PWID cluster members minus the proportion of MSM cluster members. Observations are coloured by cluster risk composition, such that the reddest clusters have the highest proportion of MSM individuals and the bluest clusters have the highest proportion PWID individuals. Adjusted cluster growth refers to the amount of cluster growth, normalized by cluster size and new diagnoses during a given time period. Only clusters that experienced growth during a given time period are shown. B) Bars represent total adjusted cluster growth seen in all clusters associated with each risk factor in a given time period. In this analysis, binary classification of cluster risk factors was done by labelling clusters with a risk composition of -0.5 or less as MSM and clusters with a risk composition of 0.5 or more as PWID. Ambiguous clusters in between these thresholds, marked by open circles, were not included in the group totals. Closed circles represent clusters contributing to the risk group totals. Black horizontal lines represent the median adjusted cluster growth of the closed circles associated with each risk group in each time period.

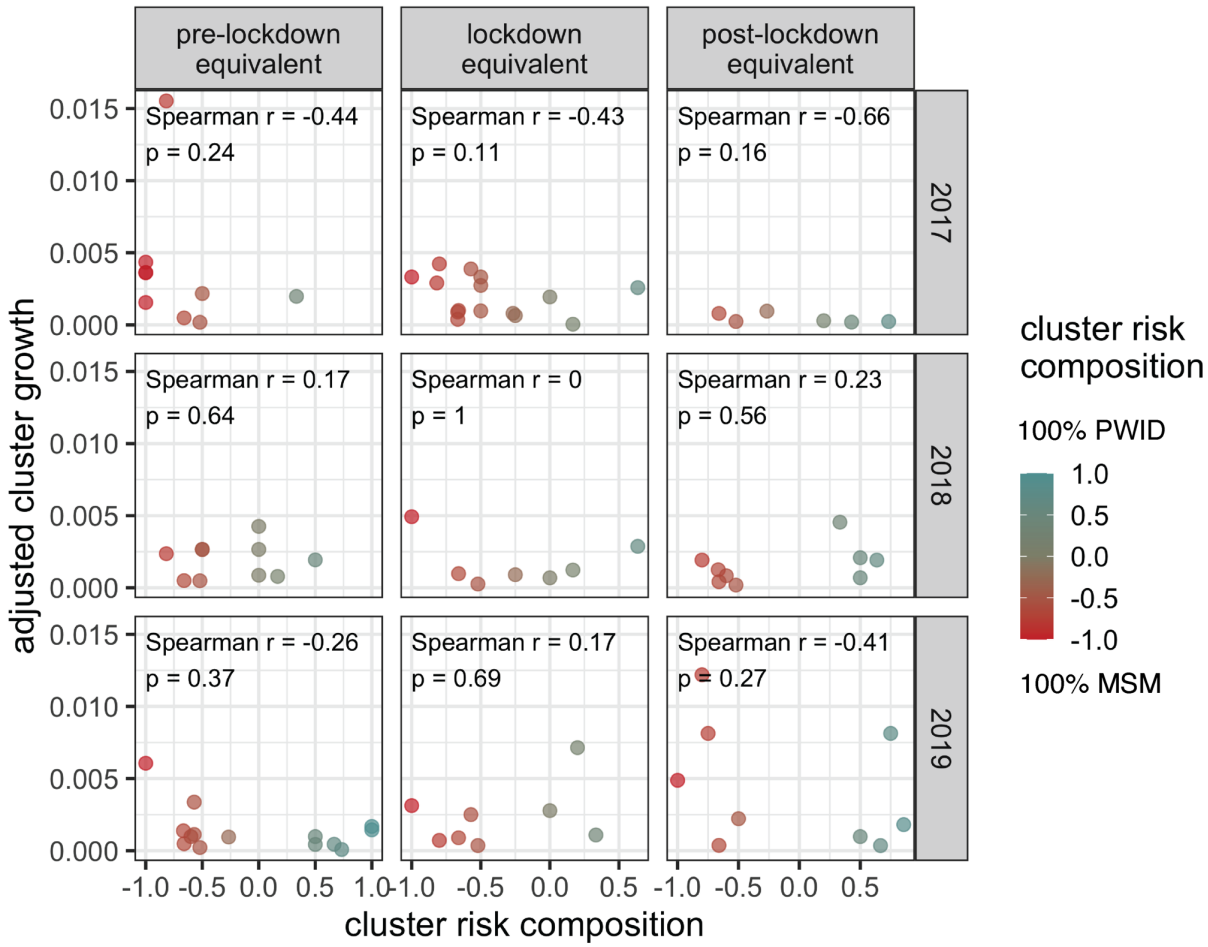

Figure 3.3 Differences in adjusted cluster growth by cluster risk factor composition in 2017 to 2019. Adjusted cluster growth versus cluster risk composition, defined as the proportion of PWID cluster members minus the proportion of MSM cluster members. Observations were selected from periods between the same dates as the time periods studied in 2020, creating three "equivalent" time periods. Observations are coloured by relative risk proportion, such that the red-hued clusters have the highest proportion of MSM and the blue-hued clusters have the highest proportion PWID. Adjusted cluster growth refers to the number of new cases in a cluster, normalized by cluster size and total new diagnoses during a given time period.

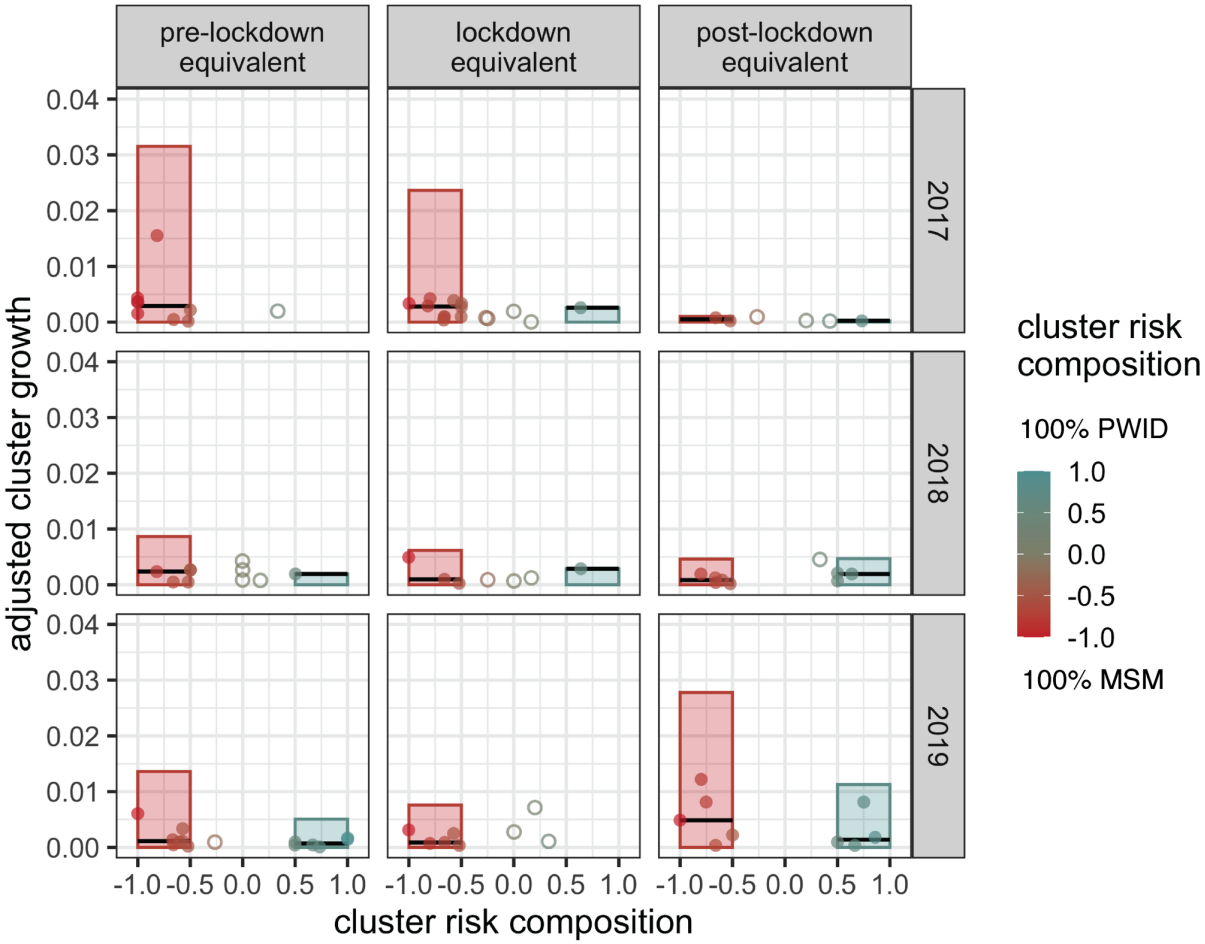

Figure 3.4. Differences in total adjusted cluster growth by risk factor composition in 2017 to 2019. Bars represent the total adjusted cluster growth seen in all clusters associated with each risk factor in a given time period. Observations were selected from periods between the same dates as the time periods studied in 2020, creating three "equivalent" time periods. Binary classification of cluster risk factors was done by labelling all clusters with a proportion of PWID minus proportion MSM of -0.5 or less as MSM and all clusters with a proportion of PWID minus proportion MSM of 0.5 or more as PWID. Ambiguous clusters in between these thresholds were not included in the group totals. Closed circles represent clusters contributing to the risk group totals. Black horizontal lines represent the median adjusted cluster growth of the closed circles associated with each risk group in each time period.

Looking at individual clusters on a more long-term scale reveals similar trends – of all the clusters that grew by four or more cases between March 21st, 2020 and June 4th, 2021, those with higher PWID risk composition generally underwent greater percentage growth (Figure 3.5). Furthermore, the only new clusters identified during this time display PWID-rich risk composition (0.75, 1). Notably, many of these clusters continued to experience elevated growth

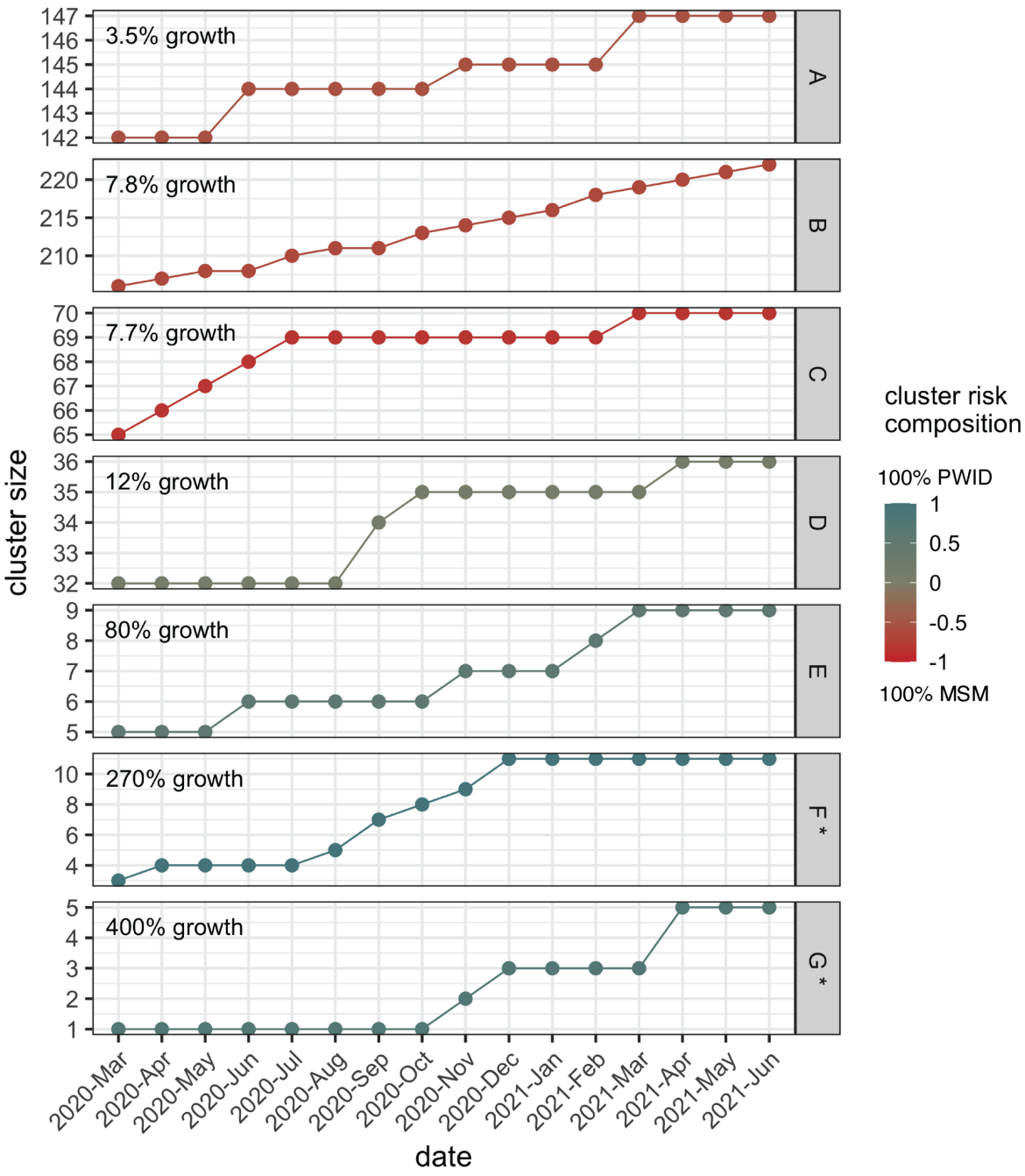

Figure 3.5 Long-term cluster growth for all clusters that grew by four cases or more following lockdown in March 2020 until June 2021. The plots are shown in ascending order, based on the percent increase in cluster size seen between March 1st, 2020 and June 4th, 2021. Unlike the previous figures, raw unadjusted cluster growth is shown. Colour indicates cluster risk composition of reported risk factors within a cluster, specifically the proportion of MSM subtracted from the proportion of PWID, such that the red-hued clusters have the highest proportion of MSM individuals and the blue-hued clusters have the highest proportion PWID individuals. Arbitrary cluster identification labels are shown in the strip label. The clusters marked with an asterisk were initially identified after the implementation of lockdown restrictions.

well beyond the initial period of instability in health service availability, indicating that the effects of such gaps can be long-term and difficult to counterbalance, thus expanding the potential for negative impact. It is also important to note that although 38 clusters ranging in risk composition experienced some level of sampled growth during the period between March 21st, 2020 and June 4th 2021, 176 clusters also ranging in risk composition experienced no observed growth at all, indicating that sampled growth is not purely a function of time, at least in well-controlled epidemic settings such as BC (Figure 3.6).

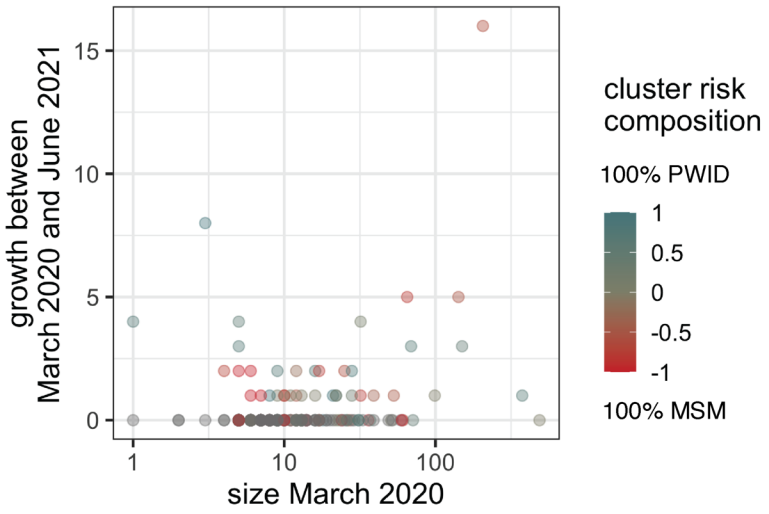

Figure 3.6 Initial cluster size versus observed growth. Each dot represents a cluster. Observations are coloured by cluster risk composition, such that the reddest clusters have the highest proportion of MSM individuals and the bluest clusters have the highest proportion PWID individuals. Initial size was measured on March 21st, 2020. Growth was measured between March 21st, 2020 and June 4th, 2021.

The level of transmission occurring in association with MSM populations versus PWID populations was further explored via calculation of the number of cluster-associated branching events during each time period. When adjusted by cluster size and the total number of new diagnoses in each time period, the total number of putative transmissions associated with clusters showing higher PWID composition increased markedly during lockdown and continued to

increase post-lockdown, although median adjusted cluster growth decreased post-lockdown (Figure 3.7A). Analysis of individual clusters reveals the post-lockdown increase in branching events to be driven by a single rapidly growing cluster, while the remainder return to approximately pre-lockdown levels (Figure 3.7A). The levels of branching events seen during lockdown and post-lockdown were unmatched during the equivalent time periods in the previous three years (Figure 3.7A, 3.8). Clusters showing higher MSM composition were linked to similar numbers of branching events across the three time periods (Figure 3.7A).

Accelerated growth in clusters characterized by PWID versus MSM populations was further demonstrated by comparison of total median change in lineage-level diversification rates shown by cluster members following the announcement of lockdown restrictions, relative to cluster size and the total number of new diagnoses (Figure 3.7B). Total median adjusted change in diversification rate in PWID-associated clusters demonstrated a stark peak during lockdown, reaching a level 4.7 times higher than previously seen in either group of clusters in the equivalent time periods over the preceding three years (Figure 3.7B, 3.9). Conversely, although total change in diversification rate for MSM-associated clusters did not differ drastically between time periods, it did dip slightly during lockdown (Figure 3.7B).

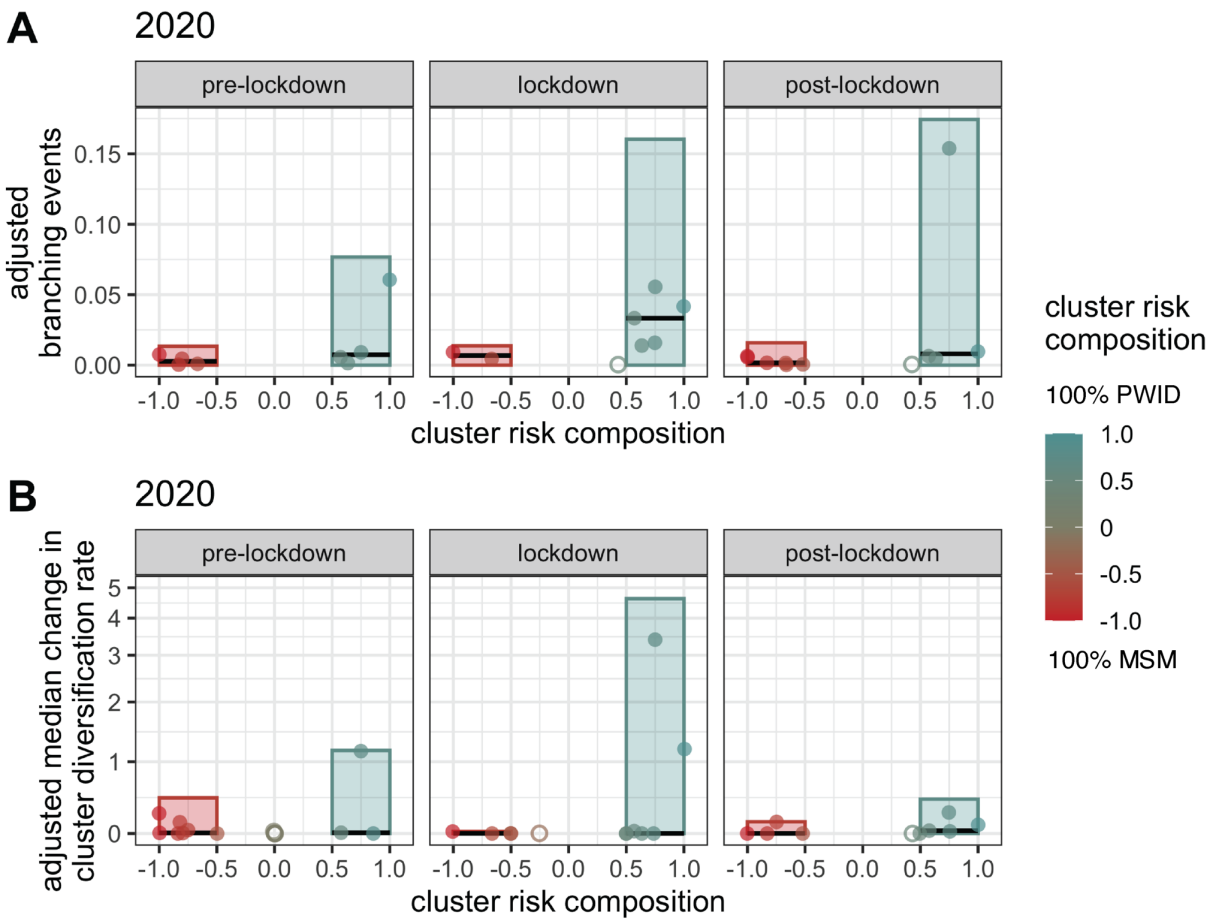

Figure 3.7 Branching events and cluster change in diversification rate by risk factor composition. Bars represent the total number of A) total daily median branching events inferred to be associated with clusters of each risk factor, normalized by cluster size and new diagnoses during a given time period or B) total cluster median change in individual diversification rate between the beginning and end dates of a given time period, adjusted for cluster size and new diagnoses in that time period. Only non-zero values are shown. Binary classification of cluster risk factors was done by labelling clusters with a risk composition of -0.5 or less as MSM and those with a risk composition of 0.5 or more as PWID. Ambiguous clusters in between these thresholds, marked by open circles, were not included in the group totals. Closed circles represent clusters contributing to the risk group totals. Black horizontal lines represent the median of the closed circles associated with each risk group in each time period. In order to capture the branching events more likely to be associated with a certain risk factor, each event was assigned the risk factor composition of the cluster its descendants were members of, effectively linking each branching event to a cluster.

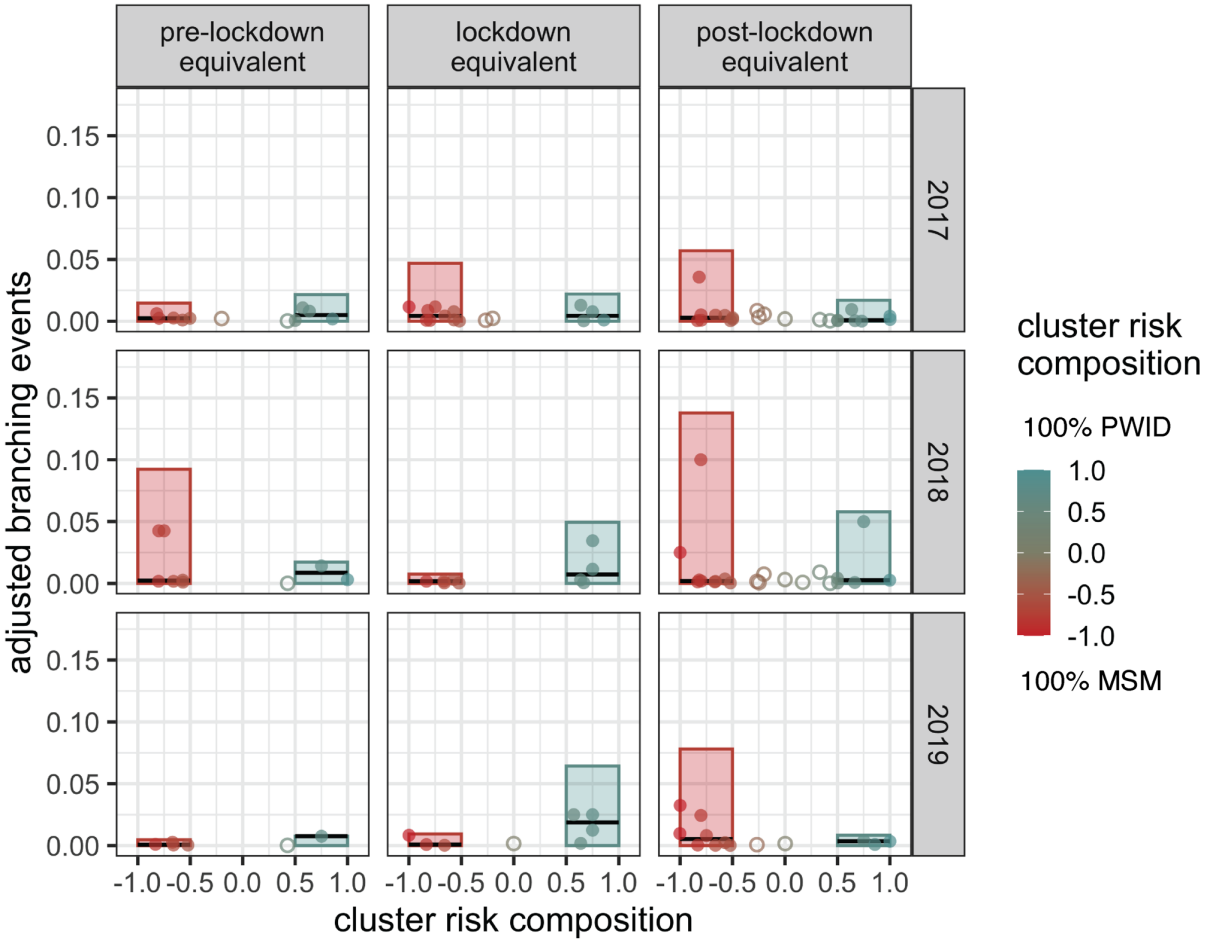

Figure 3.8 Branching events in 2017 to 2019 by risk factor. Bars represent the total number of daily median branching events inferred to be associated with clusters of each risk factor, normalized by cluster size and new diagnoses during a given time period. Observations were selected from periods between the same dates as the time periods studied in 2020, creating three "equivalent" time periods. In order to capture the branching events more likely to be associated with a certain risk factor, each event was assigned the risk factor composition of the cluster its descendants were members of. Following this, binary classification of cluster risk factors was done by labelling events assigned a risk composition of -0.5 or less as MSM and those with a risk composition of 0.5 or more as PWID. Ambiguous events assigned risk composition in between these thresholds were not included in the group totals. Closed circles represent clusters linked to events contributing to the risk group totals. Black horizontal lines represent the median of the closed circles associated with each risk group in each time period.

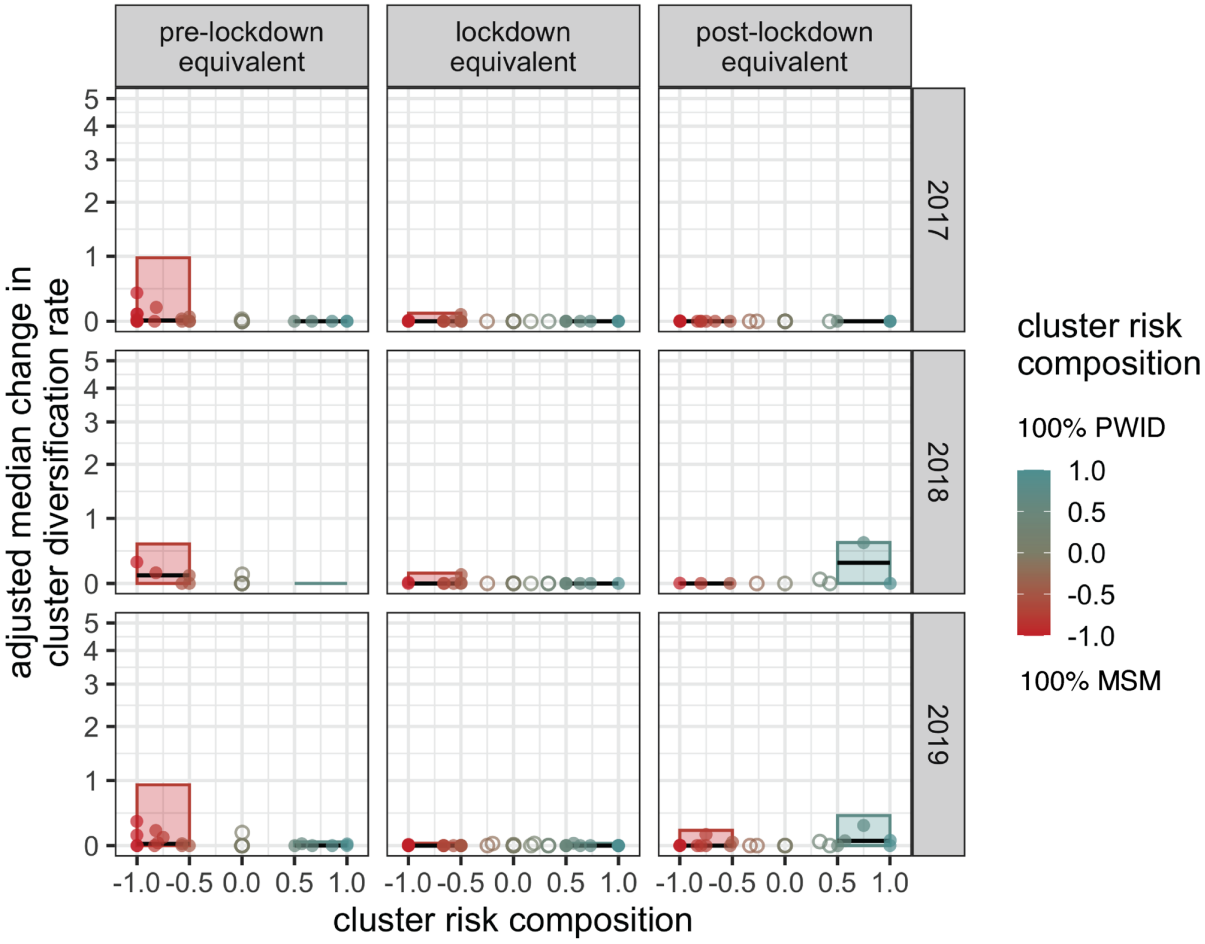

Figure 3.9 Cluster change in diversification rates within each time period in 2017 to 2019, by risk factor composition. Cluster median change in individual diversification rate between the beginning and end dates of a given time period, adjusted for cluster size and new diagnoses in that time period. Observations were selected from periods between the same dates as the time periods studied in 2020, creating three "equivalent" time periods. Binary classification of cluster risk factors was done by labelling clusters with a risk composition of -0.5 or less as MSM and those with a risk composition of 0.5 or more as PWID. Ambiguous clusters in between these thresholds were not included in the group totals. Closed circles represent clusters contributing to the risk group totals. Black horizontal lines represent the median of the closed circles associated with each risk group in each time period.

3.4 Discussion

Our results support the idea that public health measures aiming to reduce transmission of SARS-CoV-2 early in the pandemic resulted in an increase in time spent at home, coinciding with an unintended significant reduction in engagement in HIV prevention and management

services. Our analyses further reveal increased transmission following the implementation of said public health measures in a limited number of PWID-associated transmission clusters. These clusters showed peaks in growth, increased number of phylogenetically-derived branching events, and elevate cluster median change in individual viral diversification rates during the lockdown period.

An important caveat of this study is that the dataset consists of one sequence for each new diagnosis, not for each new transmission. The missing data, which may be at an increased proportion relative to pre-pandemic levels[88], means that our approximations of transmission are uncertain and likely to be underestimates. Furthermore, the effect of under-sampling may have greater impact on the observed growth of smaller clusters versus larger clusters, as the likelihood of capturing members of a cluster increases with its size. Another possible source of bias stems from the fact that both clusters and the lineage-level diversification rates used to describe them are phylogenetically derived. By definition, a cluster is composed of at least five individuals close in phylogenetic distance, meaning that clusters will frequently demonstrate rapid growth or increase in diversification rate relative to their size at the time of initial detection. Although these changes may truly represent rapid transmission, they may also indicate pockets of successful contact tracing that do not fully describe transmission dynamics. Additionally, differences or pandemic-related changes in contact tracing success may have had differential influence on key population sampling rates. Despite these factors, the level of transmission detected in several key population clusters remains concerning. A second caveat is that due to the fact that sequences were collected as part of routine clinical care, the dates associated with the sequences relate to the date of first detectable viral load rather than the date of diagnosis or the date of infection and thus may introduce some uncertainty in coalescent analyses in terms of the timing of

transmissions. Finally, although we aimed to consider risk factor overlap via cluster risk composition, increases in overlapping risk behaviours linked to pandemic pressures (eg. increased risky sex among PWID[78]) may not necessarily be captured by the dataset.

Differential transmission trends between MSM and PWID clusters here identified are likely due to differences in the risk-behaviour patterns and medical supports required by individuals in these populations. While many MSM have been shown to reduce behaviour associated with possible transmission as a response to the pandemic and its related public health measures[72,73], PWID have shown increases in transmission-related behaviours[60,75-77]. A modelling study focused on the impacts of COVID-19 on the MSM population further supports the idea that opposing trends in new infections may result from different levels of risk-behaviour[89]. The study found that a 25% reduction in sexual partners resulted in a 12.2% drop in new HIV infections over the following year, but in the absence of changes to sexual behaviour, the combined effect of disruptions to prevention-related services and behaviours was a 10.5% increase in new HIV infections[89]. Similarly, a recent report from West Virginia, USA showed that the 2018 suspension of a county syringe service program and COVID-19-related closures to other services needed by PWID were followed notable local increases in HIV diagnoses[90]. Another possible reason for differences in transmission between key populations is that although all groups experienced reductions in the availability of the services they access, services such as safe injection sites are designed to be accessed with much greater frequency than other services such as clinics or testing sites, meaning the daily impact of closure or reduced capacity could accumulate much faster.

Evidence from other locations indicates that when restrictions are minimized, adjusted or adapted to, the reduction in access to services needed by PWID may be smaller. In Sweden,

where the initial response to COVID-19 was much less restrictive than in other countries, HIV tests did decrease, but multiple measures of engagement with needle exchange programs remained stable or increased; 85.3% of participants reported sufficient access to safe injection equipment during the COVID-19 pandemic and only 10.3% reported less access to out-patient appointments[91]. This suggests that although demand for support services during the initial months of the pandemic may have increased, the absence of a Swedish lockdown minimized interference with the medical needs of the population. Similarly, in Austria, regulations regarding opioid substitution therapy (OST) prescriptions were temporarily eased during lockdown in order to allow continued adherence, a choice thus far followed by no observed change in OST-related consumption patterns[92]. However, minimizing or targeted loosening of restrictions may be unfeasible depending on the level of government cooperation and pandemic severity. A 2020 survey found that syringe service programs in the USA are maintaining service provision by prepacking supplies before distribution, providing delivery services and increasing the amount of supplies given out at once[67].

Although the long-term effects of disruptions to engagement with HIV care services are yet to be seen, a multitude of mathematical modelling studies estimate the negative impacts to be substantial[93-96]. An estimated 10% to 60% increase in HIV-related deaths could stem from disruptions to ART[93,94] and viral suppression[95]. Increases in HIV infection rates ranging from 5% to 15.7% have also been predicted in relation to reductions in health services[96] and condom use[95]. Due to the exponential nature of viral transmission, increase of any magnitude in HIV infections can have downstream effects requiring much more resources to control than would be necessary for primary prevention and thus preserving engagement with HIV care is crucial to resource-efficient protection that limits the harm experienced by the at-risk community.

3.5 Conclusions

Maintaining engagement with HIV prevention and management services is crucial to preventing regression in epidemic control and unnecessary detriment to at-risk populations. In particular, differing pressures, behaviours and needs between key populations should be carefully considered prospectively, ideally at the point of restriction design, but at minimum as a rapid response to restriction implementation. Increased vigilance and innovative targeted solutions are critical to offset potential negative impacts on HIV treatment and prevention stemming from not only COVID-19 restrictions, but also restrictions related to future pandemics or other major public health events.

Chapter 4: Conclusion

4.1 Analysis of results in the context of current research

Overall, the findings presented in this thesis demonstrate the value of phylogenetic methods in monitoring HIV transmission. Results in Chapter 2 demonstrate that phylogenetically derived lineage-level diversification rates are comparable to non-phylogenetic measures of prioritization in separating priority clusters from the remainder when considering empirical data and frequently highlight clusters more strongly correlated with future transmission and clusters that result in more downstream transmissions when considering simulated data. These analyses intentionally include non-phylogenetic prioritization measures used in other recent literature[37,97] in order to facilitate direct comparison. Furthermore, these findings are in concordance with previous research that showed lineage-level diversification rates to be predictive of future transmission[44], although not in the context of transmission clusters. Results also showed an additional advantage of diversification rate measures, which is that they are frequently more robust to downsampling. Recent research on lineage-level diversification rates[45] and terminal branch lengths[40] reports similar robustness in response to downsampling, which taken together with our findings perhaps suggests that phylogenetically-derived measures, and in particular those weighted towards the present, are more robust in their recovery of ongoing transmission trends in the face of missing data.

Results in Chapter 3 provided phylogenetic evidence of changing HIV transmission trends in association with the COVID-19 pandemic and its related restrictions. Changes in transmission related to reductions in health service capacity and availability have also been documented in relation to other infectious diseases such as malaria[98], syphilis[99], chlamydia and

gonorrhea[100,101]. Disruptions likely to lead to increased transmission of hepatitis B virus (HBV) and HCV have also been observed[81], although direct quantification of transmission changes has yet to be shown. Furthermore, recent research suggests that the impact of reductions in health service availability may be greater than the impact of COVID-19 itself, in terms of deaths[102]. Together, these findings suggest that potential downstream impacts of restrictions may be both widespread and extensive, thus necessitating careful consideration by public health teams and health service providers when implementing and adapting to restrictions

Recent reports show that the BC HIV epidemic has become relatively well-controlled[12], partially due to the use of transmission monitoring. However, as demonstrated by the impacts of the COVID-19 pandemic, transmission dynamics can be influenced by unexpected and unfamiliar external forces, and the ability to reveal a comprehensive picture of transmission trends over time is highly valuable. Furthermore, even in the absence of extenuating circumstances, transmitting groups persist, making the exploration of refined prioritization measures a worthwhile pursuit.

4.2 Evaluation of hypotheses

Both hypotheses outlined at the outset of this work are supported by the findings described here. The first hypothesis was that HIV transmission cluster prioritization based on phylogenetically derived lineage-level diversification rates would be at least as effective as commonly used non-phylogenetic measures in stratifying clusters by future growth potential, without need for historical data or subjective interpretation. This statement is in agreement with the results described in Chapter 2, whereby lineage-level diversification rate based measures were not only found to be equally as effective as commonly used non-phylogenetic measures in the separation

of high priority clusters from the remainder, but also found to highlight clusters more closely associated with future growth and clusters with more downstream transmissions. The second hypothesis was that following implementation of SARS-CoV-2 restrictions and reduced access to HIV management and prevention services in BC, key populations at risk for HIV would demonstrate differential trends in rates of transmission detectable via phylogenetic analyses. This is congruent with the findings outlined and discussed in Chapter 3, which demonstrate differential changes in transmission between MSM-associated and PWID-associated clusters, as quantified by cluster growth, branching event timing and change in lineage-level diversification rates.

4.3 Significance and contribution

This research contributes new insights to the field of HIV transmission monitoring and is consistent with and supportive of previous findings. The simulation analyses described here form the first evaluation of lineage-level diversification rates as a transmission cluster prioritization measure in the absence of biases such as differential cluster intervention and incomplete sampling. Furthermore, as discussed in Section 4.1, the findings from our simulated data concur with results previously published by McLaughlin *et al*.[44,45] and Moshiri *et al*.[40], thus contributing to the body of literature that demonstrates the value and advantages of employing phylogenetic measures in transmission monitoring.

The results presented here also form the first predominantly phylogenetically-informed quantification of differential impacts of SARS-CoV-2 related restrictions on HIV transmission between key populations. By demonstrating the disproportionate negative impacts experienced by PWID-associated populations, we offer evidence crucial to the design of both counteractive

strategies and the implementation of future restrictions. Additionally, these findings serve to alert other regions to the possibility of similar outcomes in their own HIV-transmitting populations and provide a straightforward, replicable method of quantifying changes in transmission across groups associated with differing risk factors.

4.4 Strengths and limitations

The major strengths of this research are its underlying dataset, it's generalizability and it's novelty. As the BC-CfE has collected sequence data and linked metadata from all individuals receiving drug-resistance testing since 1996, the number of individuals with viral sequences and the sampling proportion of the dataset are uncommonly high relative to other sampled epidemics. This is of particular advantage not only due to the large sample size, but also because one of the primary sources of error during phylogenetic tree inference is missing taxa[103]. The epidemic simulations also confer strength to our findings, as they provide a platform for evaluation of different prioritization measures where the clusters with the highest growth potential are known and biases including uneven sampling and differential intervention are removed. Furthermore, simulation allowed easy adjustment of parameters, such that several possible epidemic scenarios with different characteristics were able to be used as platforms for evaluation, conferring greater transferability to the results. Finally, particularly in the case of Chapter 3, the analyses conducted reveal unaddressed pandemic-related gaps in HIV prevention in BC that have not previously been phylogenetically demonstrated, making this work a valuable piece of evidence in the construction of counteractive public health strategies.

One important limitation to note is that because the sequence dataset was collected for the purpose of drug resistance testing, the dates associated with each of the sequences reflect the date

of the first detectable viral load, not the date of diagnosis or infection and thus may introduce some uncertainty into processes that rely on date information such as rooting or branching event timing. Furthermore, in the version of the dataset that extends beyond the end of 2019, reduced sampling due to the effects of the SARS-CoV-2 pandemic introduces further uncertainty into tree inference and quantifications of cluster growth, branching events and lineage-level diversification rates. Another potential source of inaccuracy is the risk factor data, which uses broad labels to categorize the context of transmission, and can thus inappropriately describe complex risk factor combinations or risk factors that may have changed over time. A further caveat to consider is that although there are advantages to the use of simulated data, its dynamics are generated by drawing from fixed distributions and models and our simulation parameters assume a certain level of predictability that may not always be in line with fluctuations and exceptions occurring in the real world, thus resulting in data that approximates real circumstances in general rather than providing an exact replica of the truth. Additionally, the random downsampling undertaken to imitate reduced sampling proportion will not provide an exact recapitulation of natural sampling bias, and the true effects of lower sampling proportion may differ from our findings.

4.5 Potential applications and future work

The results presented in this thesis could be built upon in several ways. Transmission cluster prioritization methods could potentially be further refined via exploration of a model that combines multiple prioritization measures, including phylogenetic measures such as lineage-level diversification rate. Including multiple measures and taking other supporting knowledge into account may be able to more accurately reflect the intricacies of transmission dynamics, thus

facilitating further optimization of prioritization processes. Further study could also investigate the use of phylogenetic prioritization measures like lineage-level diversification rate to highlight subpopulations within larger clusters that may be transmitting more rapidly than the remainder of the cluster. This within-cluster prioritization could be a particularly powerful approach when considering large clusters comprising hundreds of individuals. Furthermore, now that a reasonable set of simulation parameters designed to mimic the BC epidemic have been defined, barriers to further exploration of epidemic trends in the province via simulated data are reduced. Additionally, the approach to quantifying changes in cluster transmission over time described here could be applied to HIV epidemics in other regions, in order to identify possible disparities in the fit of care provision during the SARS-CoV-2 pandemic. Finally, the same approach may also be useful in quantifying similar outcomes in the case of future pandemics or other events resulting in major public health restrictions.

References

1 Christaki, E., Marcou, M. & Tofarides, A. Antimicrobial Resistance in Bacteria: Mechanisms, Evolution, and Persistence. *J Mol Evol* **88**, 26-40, doi:10.1007/s00239-019-09914-3 (2020).

2 Lampejo, T. Influenza and antiviral resistance: an overview. *Eur J Clin Microbiol Infect Dis* **39**, 1201-1208, doi:10.1007/s10096-020-03840-9 (2020).

3 Clutter, D. S., Jordan, M. R., Bertagnolio, S. & Shafer, R. W. HIV-1 drug resistance and resistance testing. *Infect Genet Evol* **46**, 292-307, doi:10.1016/j.meegid.2016.08.031 (2016).

4 Magambo, B. *et al.* The arrival of untreatable multidrug-resistant HIV-1 in sub-Saharan Africa. *AIDS* **28**, 1373-1374, doi:10.1097/QAD.0000000000000216 (2014).

5 Gunthard, H. F. *et al.* Human Immunodeficiency Virus Drug Resistance: 2018 Recommendations of the International Antiviral Society-USA Panel. *Clin Infect Dis* **68**, 177-187, doi:10.1093/cid/ciy463 (2019).

6 Semenza, J. C. & Suk, J. E. Vector-borne diseases and climate change: a European perspective. *FEMS Microbiol Lett* **365**, doi:10.1093/femsle/fnx244 (2018).

7 Wilkinson, J. L. *et al.* Pharmaceutical pollution of the world's rivers. *Proc Natl Acad Sci U S A* **119**, doi:10.1073/pnas.2113947119 (2022).

8 McMichael, C. Climate change-related migration and infectious disease. *Virulence* **6**, 548-553, doi:10.1080/21505594.2015.1021539 (2015).

9 Booth, M. Climate Change and the Neglected Tropical Diseases. *Adv Parasitol* **100**, 39-126, doi:10.1016/bs.apar.2018.02.001 (2018).

10 Faria, N. R. *et al.* HIV epidemiology. The early spread and epidemic ignition of HIV-1 in human populations. *Science* **346**, 56-61, doi:10.1126/science.1256739 (2014).

11 World Health Organization. HIV/AIDS Fact Sheet. (2021).

12 Lima, V. D. *et al.* The Impact of Treatment as Prevention on the HIV Epidemic in British Columbia, Canada. *Curr HIV/AIDS Rep* **17**, 77-87, doi:10.1007/s11904-020-00482-6 (2020).

13 Amon, J. J. The political epidemiology of HIV. *J Int AIDS Soc* **17**, 19327, doi:10.7448/IAS.17.1.19327 (2014).

14 UNAIDS. Making the Law Work for the HIV Response: a snapshot of selected laws that support or block universal access to HIV prevention, treatment, care and support. (2010).

15 Cohen, M. S. *et al.* Prevention of HIV-1 infection with early antiretroviral therapy. *N Engl J Med* **365**, 493-505, doi:10.1056/NEJMoa1105243 (2011).

16 Rodger, A. J. *et al.* Sexual Activity Without Condoms and Risk of HIV Transmission in Serodifferent Couples When the HIV-Positive Partner Is Using Suppressive Antiretroviral Therapy. *JAMA* **316**, 171-181, doi:10.1001/jama.2016.5148 (2016).

17 Montaner, J. S. *et al.* Expansion of HAART coverage is associated with sustained decreases in HIV/AIDS morbidity, mortality and HIV transmission: the "HIV Treatment as Prevention" experience in a Canadian setting. *PLoS One* **9**, e87872, doi:10.1371/journal.pone.0087872 (2014).

18 Poon, A. F. *et al.* The impact of clinical, demographic and risk factors on rates of HIV transmission: a population-based phylogenetic analysis in British Columbia, Canada. *J Infect Dis* **211**, 926-935, doi:10.1093/infdis/jiu560 (2015).
19 Nosyk, B. *et al.* Relative effects of antiretroviral therapy and harm reduction initiatives on HIV incidence in British Columbia, Canada, 1996-2013: a modelling study. *Lancet HIV* **4**, e303-e310, doi:10.1016/S2352-3018(17)30045-0 (2017).
20 Lima, V. D. *et al.* Can the combination of TasP and PrEP eliminate HIV among MSM in British Columbia, Canada? *Epidemics* **35**, 100461, doi:10.1016/j.epidem.2021.100461 (2021).
21 Bennett, D. E. *et al.* Drug resistance mutations for surveillance of transmitted HIV-1 drug-resistance: 2009 update. *PLoS One* **4**, e4724, doi:10.1371/journal.pone.0004724 (2009).
22 Lima, V. D. *et al.* Progress towards the United Nations 90-90-90 and 95-95-95 targets: the experience in British Columbia, Canada. *J Int AIDS Soc* **20**, doi:10.1002/jia2.25011 (2017).
23 Volz, E. M., Koelle, K. & Bedford, T. Viral phylodynamics. *PLoS Comput Biol* **9**, e1002947, doi:10.1371/journal.pcbi.1002947 (2013).
24 Bedford, T., Cobey, S., Beerli, P. & Pascual, M. Global migration dynamics underlie evolution and persistence of human influenza A (H3N2). *PLoS Pathog* **6**, e1000918, doi:10.1371/journal.ppat.1000918 (2010).
25 Fraser, C. *et al.* Pandemic potential of a strain of influenza A (H1N1): early findings. *Science* **324**, 1557-1561, doi:10.1126/science.1176062 (2009).
26 Pybus, O. G. *et al.* The epidemic behavior of the hepatitis C virus. *Science* **292**, 2323-2325, doi:10.1126/science.1058321 (2001).
27 Brunker, K. *et al.* Elucidating the phylodynamics of endemic rabies virus in eastern Africa using whole-genome sequencing. *Virus Evol* **1**, vev011, doi:10.1093/ve/vev011 (2015).
28 Volz, E. M., Kosakovsky Pond, S. L., Ward, M. J., Leigh Brown, A. J. & Frost, S. D. Phylodynamics of infectious disease epidemics. *Genetics* **183**, 1421-1430, doi:10.1534/genetics.109.106021 (2009).
29 McLaughlin, A. *et al.* Early and ongoing importations of SARS-CoV-2 in Canada. *medRxiv*, 2021.2004.2009.21255131, doi:10.1101/2021.04.09.21255131 (2021).
30 Zanini, F., Puller, V., Brodin, J., Albert, J. & Neher, R. A. In vivo mutation rates and the landscape of fitness costs of HIV-1. *Virus Evol* **3**, vex003, doi:10.1093/ve/vex003 (2017).
31 Eddie C. Holmes , S. N., Andrew Rambaut , Geoff P. Garnett and Paul H. Harvey. Revealing the history of infectious disease epidemics through phylogenetic trees. *Philos Trans R Soc Lond B Biol Sci* **349**, doi:https://doi.org/10.1098/rstb.1995.0088 (1995).
32 Poon, A. F. Impacts and shortcomings of genetic clustering methods for infectious disease outbreaks. *Virus Evol* **2**, vew031, doi:10.1093/ve/vew031 (2016).
33 Gillespie, J. Rates of Molecular Evolution. *Annual Review of Ecology Systematics* **17**, 637-635 (1986).
34 Balaban, M., Moshiri, N., Mai, U., Jia, X. & Mirarab, S. TreeCluster: Clustering biological sequences using phylogenetic trees. *PLoS One* **14**, e0221068, doi:10.1371/journal.pone.0221068 (2019).

35 Dennis, A. M. *et al.* Phylogenetic insights into regional HIV transmission. *AIDS* **26**, 1813-1822, doi:10.1097/QAD.0b013e3283573244 (2012).
36 Oster, A. M. *et al.* Identifying Clusters of Recent and Rapid HIV Transmission Through Analysis of Molecular Surveillance Data. *J Acquir Immune Defic Syndr* **79**, 543-550, doi:10.1097/QAI.0000000000001856 (2018).
37 Wertheim, J. O. *et al.* Growth of HIV-1 Molecular Transmission Clusters in New York City. *J Infect Dis* **218**, 1943-1953, doi:10.1093/infdis/jiy431 (2018).
38 Little, S. J. *et al.* Using HIV networks to inform real time prevention interventions. *PLoS One* **9**, e98443, doi:10.1371/journal.pone.0098443 (2014).
39 Fisher, M. *et al.* Determinants of HIV-1 transmission in men who have sex with men: a combined clinical, epidemiological and phylogenetic approach. *AIDS* **24**, 1739-1747, doi:10.1097/QAD.0b013e32833ac9e6 (2010).
40 Moshiri, N., Smith, D. M. & Mirarab, S. HIV Care Prioritization Using Phylogenetic Branch Length. *J Acquir Immune Defic Syndr* **86**, 626-637, doi:10.1097/QAI.0000000000002612 (2021).
41 Mehta, S. R., Schairer, C. & Little, S. Ethical issues in HIV phylogenetics and molecular epidemiology. *Current opinion in HIV and AIDS* **14**, 221-226, doi:10.1097/COH.0000000000000538 (2019).
42 Jetz, W., Thomas, G. H., Joy, J. B., Hartmann, K. & Mooers, A. O. The global diversity of birds in space and time. *Nature* **491**, 444-448, doi:10.1038/nature11631 (2012).
43 Redding, D. W. & Mooers, A. O. Incorporating evolutionary measures into conservation prioritization. *Conserv Biol* **20**, 1670-1678, doi:10.1111/j.1523-1739.2006.00555.x (2006).
44 McLaughlin, A. *et al.* Detection of HIV transmission hotspots in British Columbia, Canada: A novel framework for the prioritization and allocation of treatment and prevention resources. *EBioMedicine* **48**, 405-413, doi:10.1016/j.ebiom.2019.09.026 (2019).
45 McLaughlin, A. *et al.* Concordance of HIV transmission risk factors elucidated using viral diversification rate and phylogenetic clustering. *Evol Med Public Health* **9**, 338-348, doi:10.1093/emph/eoab028 (2021).
46 Hogg, R. S. *et al.* Rates of new infections in British Columbia continue to decline at a faster rate than in other Canadian regions. *HIV Med* **14**, 581-582, doi:10.1111/hiv.12079 (2013).
47 Katoh, K. & Standley, D. M. MAFFT multiple sequence alignment software version 7: improvements in performance and usability. *Mol Biol Evol* **30**, 772-780, doi:10.1093/molbev/mst010 (2013).
48 Price, M. N., Dehal, P. S. & Arkin, A. P. FastTree 2--approximately maximum-likelihood trees for large alignments. *PLoS One* **5**, e9490, doi:10.1371/journal.pone.0009490 (2010).
49 Rambaut, A., Lam, T. T., Max Carvalho, L. & Pybus, O. G. Exploring the temporal structure of heterochronous sequences using TempEst (formerly Path-O-Gen). *Virus Evol* **2**, vew007, doi:10.1093/ve/vew007 (2016).
50 Moshiri, N., Ragonnet-Cronin, M., Wertheim, J. O. & Mirarab, S. FAVITES: simultaneous simulation of transmission networks, phylogenetic trees and sequences. *Bioinformatics* **35**, 1852-1861, doi:10.1093/bioinformatics/bty921 (2019).

51 To, T. H., Jung, M., Lycett, S. & Gascuel, O. Fast Dating Using Least-Squares Criteria and Algorithms. *Syst Biol* **65**, 82-97, doi:10.1093/sysbio/syv068 (2016).
52 Public Health Agency of Canada. Chief Public Health Officer of Canada's Report on the State of Public Health in Canada (2020).
53 Nathan, I. & Benon, M. COVID-19 relief food distribution: impact and lessons for Uganda. *Pan Afr Med J* **35**, 142, doi:10.11604/pamj.supp.2020.35.142.24214 (2020).
54 Adams, E. L., Caccavale, L. J., Smith, D. & Bean, M. K. Food Insecurity, the Home Food Environment, and Parent Feeding Practices in the Era of COVID-19. *Obesity (Silver Spring)* **28**, 2056-2063, doi:10.1002/oby.22996 (2020).
55 Evans, D. P., Hawk, S. R. & Ripkey, C. E. Domestic Violence in Atlanta, Georgia Before and During COVID-19. *Violence Gend* **8**, 140-147, doi:10.1089/vio.2020.0061 (2021).
56 Dekel, B. & Abrahams, N. 'I will rather be killed by corona than by him...': Experiences of abused women seeking shelter during South Africa's COVID-19 lockdown. *PLoS One* **16**, e0259275, doi:10.1371/journal.pone.0259275 (2021).
57 Branley-Bell, D. & Talbot, C. V. Exploring the impact of the COVID-19 pandemic and UK lockdown on individuals with experience of eating disorders. *J Eat Disord* **8**, 44, doi:10.1186/s40337-020-00319-y (2020).
58 Cheong, J. L. *et al.* The Impact of COVID-19 on Access to Parkinson's Disease Medication. *Mov Disord* **35**, 2129-2133, doi:10.1002/mds.28293 (2020).
59 Alexander, K. *et al.* The impact of COVID-19 on healthcare delivery for people who use opioids: a scoping review. *Subst Abuse Treat Prev Policy* **16**, 60, doi:10.1186/s13011-021-00395-6 (2021).
60 Croxford, S. *et al.* Preliminary indications of the burden of COVID-19 among people who inject drugs in England and Northern Ireland and the impact on access to health and harm reduction services. *Public Health* **192**, 8-11, doi:10.1016/j.puhe.2021.01.004 (2021).
61 Darcis, G., Vaira, D. & Moutschen, M. Impact of coronavirus pandemic and containment measures on HIV diagnosis. *Epidemiol Infect* **148**, e185, doi:10.1017/S0950268820001867 (2020).
62 Guo, W. *et al.* [Quick community survey on the impact of COVID-19 outbreak for the healthcare of people living with HIV]. *Zhonghua Liu Xing Bing Xue Za Zhi* **41**, 662-666, doi:10.3760/cma.j.cn112338-20200314-00345 (2020).
63 Simoes, D., Stengaard, A. R., Combs, L., Raben, D. & Euro, T. C.-i. a. c. o. p. Impact of the COVID-19 pandemic on testing services for HIV, viral hepatitis and sexually transmitted infections in the WHO European Region, March to August 2020. *Euro Surveill* **25**, doi:10.2807/1560-7917.ES.2020.25.47.2001943 (2020).
64 Santos, G. M. *et al.* Economic, Mental Health, HIV Prevention and HIV Treatment Impacts of COVID-19 and the COVID-19 Response on a Global Sample of Cisgender Gay Men and Other Men Who Have Sex with Men. *AIDS Behav* **25**, 311-321, doi:10.1007/s10461-020-02969-0 (2021).
65 Ejima, K. *et al.* HIV Testing by Public Health Centers and Municipalities and New HIV Cases During the COVID-19 Pandemic in Japan. *J Acquir Immune Defic Syndr* **87**, e182-e187, doi:10.1097/QAI.0000000000002660 (2021).

66 Spinelli, M. A. *et al.* Viral suppression rates in a safety-net HIV clinic in San Francisco destabilized during COVID-19. *AIDS* **34**, 2328-2331, doi:10.1097/QAD.0000000000002677 (2020).
67 Glick, S. N. *et al.* The Impact of COVID-19 on Syringe Services Programs in the United States. *AIDS Behav* **24**, 2466-2468, doi:10.1007/s10461-020-02886-2 (2020).
68 Weerasuria, M. *et al.* The Impact of the COVID-19 Pandemic on People Living with HIV in Victoria, Australia. *AIDS Res Hum Retroviruses* **37**, 322-328, doi:10.1089/AID.2021.0007 (2021).
69 Chow, E. P. F., Ong, J. J., Denham, I. & Fairley, C. K. HIV Testing and Diagnoses During the COVID-19 Pandemic in Melbourne, Australia. *J Acquir Immune Defic Syndr* **86**, e114-e115, doi:10.1097/QAI.0000000000002604 (2021).
70 Chow, E. P. F. *et al.* Changing the Use of HIV Pre-exposure Prophylaxis Among Men Who Have Sex With Men During the COVID-19 Pandemic in Melbourne, Australia. *Open Forum Infect Dis* **7**, ofaa275, doi:10.1093/ofid/ofaa275 (2020).
71 Kotyk, A. in *CTV News* (Vancouver, 2021).
72 Hammoud, M. A. *et al.* Physical Distancing Due to COVID-19 Disrupts Sexual Behaviors Among Gay and Bisexual Men in Australia: Implications for Trends in HIV and Other Sexually Transmissible Infections. *J Acquir Immune Defic Syndr* **85**, 309-315, doi:10.1097/QAI.0000000000002462 (2020).
73 Hyndman, I., Nugent, D., Whitlock, G. G., McOwan, A. & Girometti, N. COVID-19 restrictions and changing sexual behaviours in HIV-negative MSM at high risk of HIV infection in London, UK. *Sex Transm Infect* **97**, 521-524, doi:10.1136/sextrans-2020-054768 (2021).
74 Ablona A *et al.* Sex in the time of COVID-19: Preliminary results from a survey conducted on July 21 to August 4, 2020. (Digital Sexual Health Initiative, 2020).
75 Morin, K. A., Acharya, S., Eibl, J. K. & Marsh, D. C. Evidence of increased Fentanyl use during the COVID-19 pandemic among opioid agonist treatment patients in Ontario, Canada. *Int J Drug Policy* **90**, 103088, doi:10.1016/j.drugpo.2020.103088 (2021).
76 Holland, K. M. *et al.* Trends in US Emergency Department Visits for Mental Health, Overdose, and Violence Outcomes Before and During the COVID-19 Pandemic. *JAMA Psychiatry* **78**, 372-379, doi:10.1001/jamapsychiatry.2020.4402 (2021).
77 Slavova, S., Rock, P., Bush, H. M., Quesinberry, D. & Walsh, S. L. Signal of increased opioid overdose during COVID-19 from emergency medical services data. *Drug Alcohol Depend* **214**, 108176, doi:10.1016/j.drugalcdep.2020.108176 (2020).
78 Nguyen, T. T. *et al.* How has the COVID-19 epidemic affected the risk behaviors of people who inject drugs in a city with high harm reduction service coverage in Vietnam? A qualitative investigation. *Harm Reduct J* **19**, 6, doi:10.1186/s12954-021-00586-1 (2022).
79 Schlosser, A. & Harris, S. Care during COVID-19: Drug use, harm reduction, and intimacy during a global pandemic. *Int J Drug Policy* **83**, 102896, doi:10.1016/j.drugpo.2020.102896 (2020).
80 Genberg, B. L. *et al.* The health and social consequences during the initial period of the COVID-19 pandemic among current and former people who inject drugs: A rapid phone survey in Baltimore, Maryland. *Drug Alcohol Depend* **221**, 108584, doi:10.1016/j.drugalcdep.2021.108584 (2021).

81 Rehman, S. T., Rehman, H. & Abid, S. Impact of coronavirus disease 2019 on prevention and elimination strategies for hepatitis B and hepatitis C. *World J Hepatol* **13**, 781-789, doi:10.4254/wjh.v13.i7.781 (2021).
82 Joy, J. B. *et al.* The spread of hepatitis C virus genotype 1a in North America: a retrospective phylogenetic study. *Lancet Infect Dis* **16**, 698-702, doi:10.1016/S1473-3099(16)00124-9 (2016).
83 Overdose Response Indicator Report. (British Columbia Centre for Disease Control, 2021).
84 Google COVID-19 Community Mobility Reports. (Google LLC, 2021).
85 R: A language and environment for statistical computing (R Foundation for Statistical Computing, Vienna, Austria, 2021).
86 Nguyen, L. T., Schmidt, H. A., von Haeseler, A. & Minh, B. Q. IQ-TREE: a fast and effective stochastic algorithm for estimating maximum-likelihood phylogenies. *Mol Biol Evol* **32**, 268-274, doi:10.1093/molbev/msu300 (2015).
87 Kalyaanamoorthy, S., Minh, B. Q., Wong, T. K. F., von Haeseler, A. & Jermiin, L. S. ModelFinder: fast model selection for accurate phylogenetic estimates. *Nat Methods* **14**, 587-589, doi:10.1038/nmeth.4285 (2017).
88 Bonett, S. *et al.* in *Conference on Retroviruses and Opportunistic Infection* (Virtual, 2022).
89 Mitchell, K. M. *et al.* Estimating the potential impact of COVID-19-related disruptions on HIV incidence and mortality among men who have sex with men in the United States: a modelling study. *medRxiv*, doi:10.1101/2020.10.30.20222893 (2020).
90 Hershow, R. B. *et al.* Notes from the Field: HIV Outbreak During the COVID-19 Pandemic Among Persons Who Inject Drugs - Kanawha County, West Virginia, 2019-2021. *MMWR Morb Mortal Wkly Rep* **71**, 66-68, doi:10.15585/mmwr.mm7102a4 (2022).
91 Lindqvist, K., Wallmofeldt, C., Holmen, E., Hammarberg, A. & Kaberg, M. Health literacy and changes in pattern of drug use among participants at the Stockholm Needle Exchange Program during the COVID-19 pandemic. *Harm Reduct J* **18**, 52, doi:10.1186/s12954-021-00499-z (2021).
92 Fuchs-Leitner, I., Yazdi, K., Gerstgrasser, N. W. & Rosenleitner, J. Developments in Drug Addiction During COVID-19-An Austrian Perspective Based on a Clinical Sample. *Front Psychiatry* **11**, 602033, doi:10.3389/fpsyt.2020.602033 (2020).
93 Hogan, A. B. *et al.* Potential impact of the COVID-19 pandemic on HIV, tuberculosis, and malaria in low-income and middle-income countries: a modelling study. *Lancet Glob Health* **8**, e1132-e1141, doi:10.1016/S2214-109X(20)30288-6 (2020).
94 Jewell, B. L. *et al.* Potential effects of disruption to HIV programmes in sub-Saharan Africa caused by COVID-19: results from multiple mathematical models. *Lancet HIV* **7**, e629-e640, doi:10.1016/S2352-3018(20)30211-3 (2020).
95 Booton, R. D. *et al.* The impact of disruptions due to COVID-19 on HIV transmission and control among men who have sex with men in China. *J Int AIDS Soc* **24**, e25697, doi:10.1002/jia2.25697 (2021).
96 Zang, X. *et al.* The Potential Epidemiological Impact of Coronavirus Disease 2019 (COVID-19) on the Human Immunodeficiency Virus (HIV) Epidemic and the Cost-effectiveness of Linked, Opt-out HIV Testing: A Modeling Study in 6 US Cities. *Clin Infect Dis* **72**, e828-e834, doi:10.1093/cid/ciaa1547 (2021).

97 Little, S. J. *et al.* Effective Human Immunodeficiency Virus Molecular Surveillance Requires Identification of Incident Cases of Infection. *Clin Infect Dis* **73**, 842-849, doi:10.1093/cid/ciab140 (2021).
98 World Health Organization. World Malaria Report 2020. (World Health Organization, 2020).
99 Stanford, K. A., Almirol, E., Schneider, J. & Hazra, A. Rising Syphilis Rates During the COVID-19 Pandemic. *Sex Transm Dis* **48**, e81-e83, doi:10.1097/OLQ.0000000000001431 (2021).
100 Pinto, C. N. *et al.* Impact of the COVID-19 Pandemic on Chlamydia and Gonorrhea Screening in the U.S. *Am J Prev Med* **61**, 386-393, doi:10.1016/j.amepre.2021.03.009 (2021).
101 De Baetselier, I. *et al.* The impact of physical restriction measures imposed during the two waves of COVID-19 on chlamydia and gonorrhea diagnoses in Belgium. Results of an sexually transmitted infection clinic. *Int J STD AIDS* **32**, 998-1003, doi:10.1177/09564624211013289 (2021).
102 Stover, J. *et al.* The risks and benefits of providing HIV services during the COVID-19 pandemic. *PLoS One* **16**, e0260820, doi:10.1371/journal.pone.0260820 (2021).
103 Roure, B., Baurain, D. & Philippe, H. Impact of missing data on phylogenies inferred from empirical phylogenomic data sets. *Mol Biol Evol* **30**, 197-214, doi:10.1093/molbev/mss208 (2013).
104 Barabasi, A. L. & Albert, R. Emergence of scaling in random networks. *Science* **286**, 509-512, doi:10.1126/science.286.5439.509 (1999).
105 Hamilton, D. T., Handcock, M. S. & Morris, M. Degree distributions in sexual networks: a framework for evaluating evidence. *Sex Transm Dis* **35**, 30-40, doi:10.1097/olq.0b013e3181453a84 (2008).
106 HIV and Sexually Transmitted Infections Report. (Clinical Prevention Services, British Columbia Centre for Disease Control, 2010).
107 Granich, R. M., Gilks, C. F., Dye, C., De Cock, K. M. & Williams, B. G. Universal voluntary HIV testing with immediate antiretroviral therapy as a strategy for elimination of HIV transmission: a mathematical model. *Lancet* **373**, 48-57, doi:10.1016/S0140-6736(08)61697-9 (2009).
108 Nosyk, B. *et al.* The cascade of HIV care in British Columbia, Canada, 1996-2011: a population-based retrospective cohort study. *Lancet Infect Dis* **14**, 40-49, doi:10.1016/S1473-3099(13)70254-8 (2014).
109 Colijn, C. & Plazzotta, G. A Metric on Phylogenetic Tree Shapes. *Syst Biol* **67**, 113-126, doi:10.1093/sysbio/syx046 (2018).

Appendix: Selection and optimization of FAVITES parameters

Simulations were performed using the FAVITES framework[50]. Initial estimates of parameter choices were iteratively refined to concurrently optimize the number of output sequences (Figure A.1), phylogeny branch lengths and structure (Figure A.2, A.5, A.6), the diversification rate (Figure A.4) distribution and the transmission cluster size distribution (Figure A.7) to best mimic the BC epidemic. Each variation on the base parameter set changes only one parameter, either the number of seed individuals (and corresponding contact network size), the length of time to begin ART, or the number of contacts each individual has within the contact network. A full list of parameter choices can be found in Table A.1.

Parameters not mentioned going forward can be assumed to follow the parameter choices and justification seen in Moshiri *et al*. 2019. In all parameter sets, the contact network was generated under a Barabási-Albert model, which generates scale-free networks reflective of the connectivity of social or sexual networks[50,104,105]. The three values chosen for the number of seed individuals were selected to represent the sum of undiagnosed plus untreated diagnosed individuals (i.e. not virologically suppressed infected population), where the diagnosed population yet to begin treatment was assumed to be approximately 15% of the total diagnosed population[12]. This assumption is based on values estimated for 2013, as this marks the middle of the simulation period. Contact network sizes corresponding to the chosen seed values, and the three values chosen for the expected degree of connection of each contact network node were selected based on 2008 estimates regarding the BC epidemic[106]. Seed selection from the contact network was conducted at random.

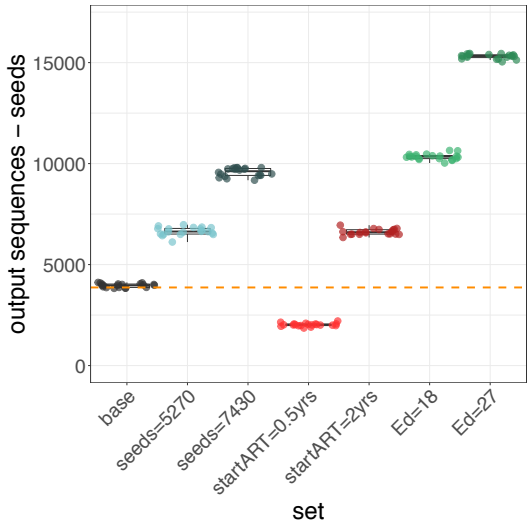

Figure A.1 Number of sequences output by each parameter set. Boxplot showing the median and IQR of the number of sequences output by each simulation parameter set, after subtraction of seed individuals and across 20 replicates. The orange dashed line indicates the target number of output sequences. As. intended, the chosen parameter sets resulted in a range of outcomes in number of output sequences, some a closer match to the empirical BC data, and some more representative of other epidemics with different characteristics. Parameter set abbreviations are as defined in Figure 2.6.

Transmissions occurred under an adapted version of the HIV-ART model described by Granich *et al*. in 2009[107]. Expected time to transition from an untreated state to a treated state was set to either 0.5, 1 or 2 years. Expected time to transition from a treated state back to an untreated state was set to 10 years, to represent BC's relatively high rate of ART retention[108].

In the BC dataset, which has been estimated to achieve approximately 75% sampling of the total prevalent population[12] 3,094 new sequences were collected in the 2009-2018 period. Thus, transmission rates were scaled such that the number of new infections generated during the simulation period for the lowest number of seeds was equal to the sum of the number of seeds plus approximately 3,868 new infections (Figure A.1).

A subset of the BC epidemic phylogeny containing only subtype B sequences collected during 2009 and onwards was used to infer parameters related to sequence evolution and mutation rates. Mutation rates were sampled from a truncated (0, ∞) normal distribution. LSD2[51]

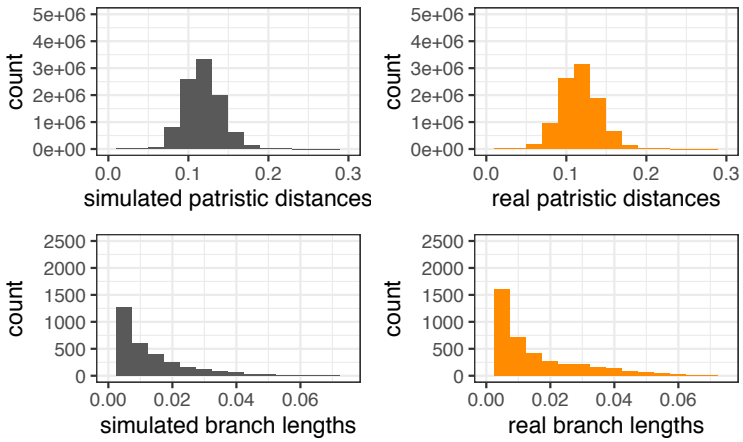

Figure A.2 Comparison of simulated to real patristic distances and branch lengths. Shown for a representative replicate of the base parameter set. Differences between real and simulated patristic distances and branch length distributions were iteratively minimized based on Jensen-Shannon Divergence (JSD) scores.

was used to determine an initial estimate of the mutation rate, which was then used in combination with patristic distance distributions to refine the location and scale parameters of the mutation rate distribution such that Jensen-Shannon Divergence (JSD) scores comparing the real and simulated patristic distance distributions were minimized (Figure A.2). The opposing subset of the BC phylogeny containing only sequences collected before 2009 was used to estimate the time to most recent common ancestor (tMRCA), as this parameter is used to build the seed tree of individuals already infected at time zero. Using LSD2, the tMRCA from the end of 2008 was estimated to be 1946. The speciation rate of the seed tree was optimized to match the accumulation of lineages over time seen in the BC dataset before 2009 (Figure A.3). Potential rate functions demonstrating exponential decay were scaled for comparison in TreeSAP and the best match was confirmed to be appropriate via visual evaluation of similarity between the median lineage through time (LTT) plot of 20 FAVITES replicates versus the BC LTT plot. Sequence evolution was set to occur under the generalized time-reversible (GTR) substitution model with gamma rate heterogeneity and the associated parameters were inferred from the post-

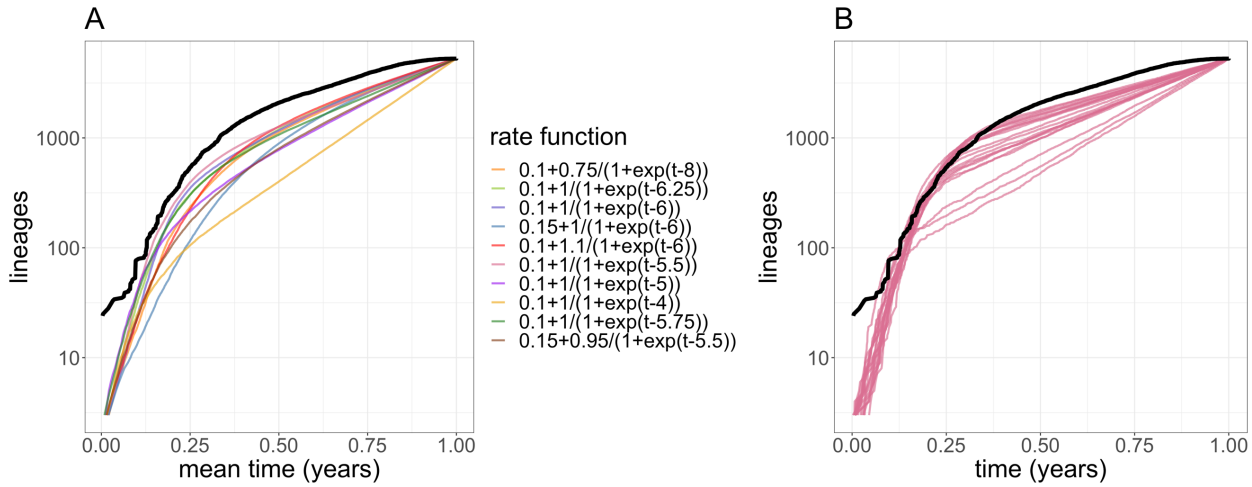

Figure A.3 Comparison of possible rate functions. A) Comparison of the mean accumulation of lineages through time (LTT) for several possible rate functions, scaled to a 1 year time period in TreeSAP. The LTT line representing the real data is shown in black. B) Accumulation of lineages through time resulting from simulation in FAVITES for the selected rate function, shown for 20 replicates. The most appropriate rate function was selected via visual evaluation of similarity between the median LTT line of 20 FAVITES replicates versus the BC LTT line.

2008 BC alignment using IQ-TREE v1.61 [86].

Sampling was done at the time of ART initiation, meaning that 100% sampling indicates 100% of diagnosed cases, not 100% of infections. Each fully sampled sequence dataset was also randomly downsampled by year to 75%, 50% and 25% of diagnoses to investigate the impact of missing data. In order to account for the variation between FAVITES runs, 20 replicates were run for each of the seven parameter sets.

Initial FAVITES parameters were selected based on the literature or inferred from the BC dataset and optimized iteratively in order to achieve a closer match to the characteristics of the BC data. As there are many characteristics to consider in tandem, some were prioritized over others. In particular, the difference between the distribution of diversification rates in the real data versus the simulated data, quantified by JSD score, was minimized (Figure A.4), as the

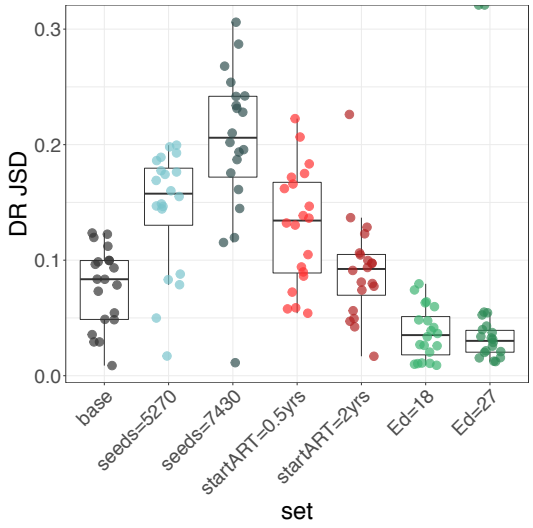

Figure A.4 Comparison of simulated to real diversification rates. Boxplot showing the median and IQR of the Jensen-Shannon Divergence (JSD) scores between the simulated and real distribution of diversification rates across 20 replicates. Differences between real and simulated lineage-level diversification rates were iteratively minimized based on JSD scores. Parameter set abbreviations are as defined in Figure 2.6.

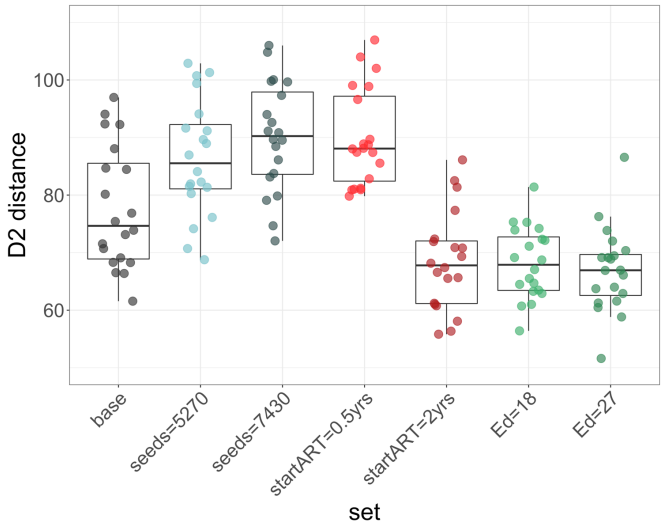

Figure A.5 Comparison of simulated tree structure to real tree structure. Difference was quantified by D2 distance[109] across 20 replicates. Boxplots show the median and IQR D2 distance. Parameter set abbreviations are as defined in Figure 2.6.

prioritization measures under study rely heavily on these values. Other characteristics considered in the optimization of parameters were the tree structure, branch lengths, root-to-tip distance, and the distribution of transmission cluster sizes (Figures A.5-7).

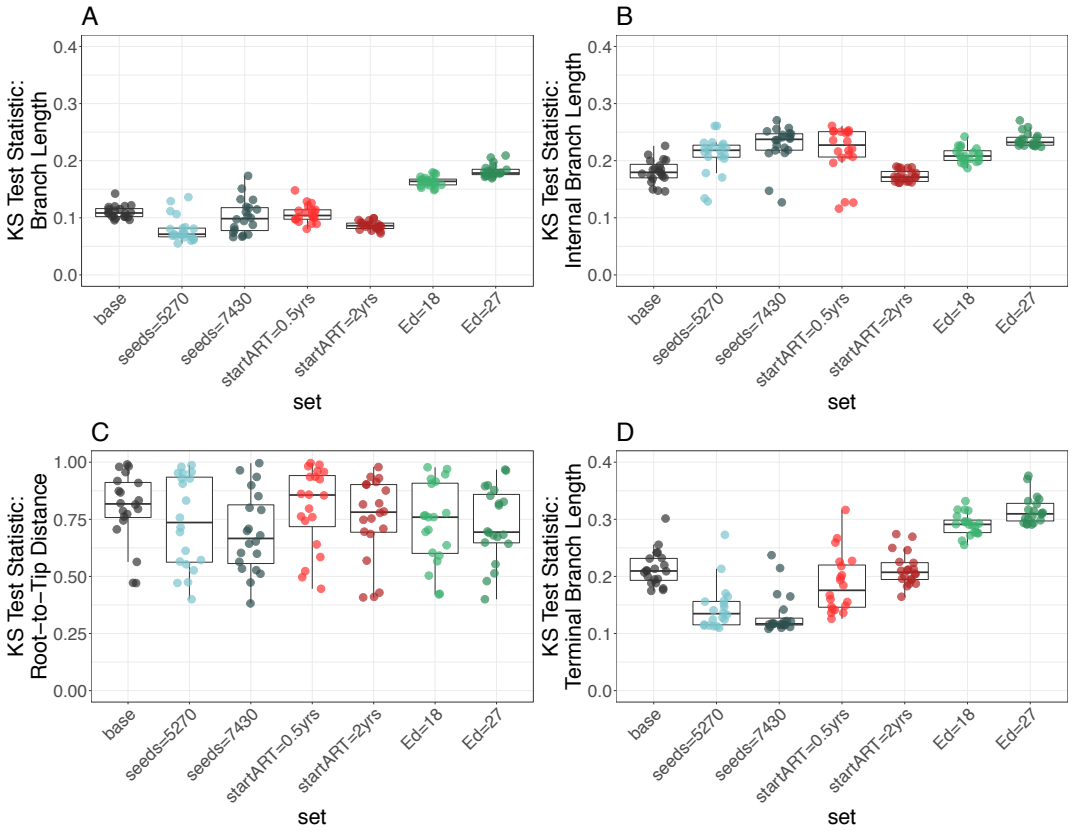

Figure A.6 Comparison of simulated to real branch lengths. Boxplots showing the median and IQR of the Kolmogorov-Smirnov test statistic evaluating the similarity of simulated versus empirical A) branch lengths, B) internal branch lengths, C) root-to-tip distance and D) terminal branch lengths. As intended, the chosen parameter sets resulted in a range of outcomes in number of output sequences, some a closer match to the empirical BC data, and some more representative of other epidemics with different characteristics. Parameter set abbreviations are as defined in Figure 2.6.

Despite efforts to capture the characteristics of the BC epidemic in our simulations, we recognize that by drawing from fixed distributions and models, our simulation parameters assume a certain level of predictability that may not always be in line with fluctuations and exceptions occurring in the real world, thus resulting in data that approximates real circumstances in general rather than providing an exact replica truth. It should also be noted that the list of prioritization measures studied here is not exhaustive and study of additional measures may allow further optimization of prioritization.

Figure A.7 Comparison of cluster size distributions. Cluster size distributions are shown for the final year of each simulated parameter set, compared to cluster size distributions from empirical data from the same year. Counts of cluster sizes represent the mean counts across 20 simulation replicates. As intended, the chosen parameter sets resulted in a range of cluster size distribution outcomes, some a closer match to the empirical BC data, and some more representative of epidemics with different characteristics. Parameter set abbreviations are as defined in Figure 2.6.

Parameter	Value
ContactNetworkGenerator	Barabasi-Albert
num_cn_nodes	(26746, 45322, 63898)
num_edges_from_new	(9, 18, 27)
SeedSelection	Random
num_seeds	(3110, 5270, 7430)
SeedSequence	VirusNonHomYuleHeightGTRGamma
seed_height	62
viral_sequence_type	HIV1-B-DNA-POL-LITTLE
seed_speciation_rate_func	0.1+1/(1+exp(t-5.5))
TransmissionTimeSample	HIVARTGranichGEMF
hiv_a1_to_a2	4.333333
hiv_a1_to_i1	0.096
hiv_a2_to_i2	0.096
hiv_i1_to_a1	(0.5, 1, 2)
hiv_i1_to_i2	8.666667
hiv_i2_to_a2	(0.5, 1, 2)
hiv_s_to_i1_by_a1	0.002
hiv_s_to_i1_by_i1	0.04
hiv_s_to_i1_by_i2	0.008
end_time	10
TreeUnit	Truncated Normal
tree_mutation_loc	0.0003
tree_mutation_scale	0.0008
tree_mutation_min	0
tree_mutation_max	Inf
SequenceEvolution	GTRGammaSeqGen
GTR state frequencies	[A: 0.395, C:0.171, T: 0.211, G:0.222]
GTR transition rates	[λ_{AC}: 1.75637, λ_{AG}: 8.32038, λ_{AT}: 0.629219, λ_{CG}: 0.71545, λ_{CT}: 8.32038, λ_{GT}: 1]
seqgen_gamma_shape	0.4237896
NodeEvolution	VirusTreeSimulator
vts_model	logistic
vts_no	1
vts_growthRate	2.851904
vts_t50	-2
TimeSample	GranichFirstART
NumTimeSample	Once

Table A.1 FAVITES simulation parameters. Parameters in bold were varied across parameter sets.